EFFECTS OF THERMAL TREATMENTS ON PERFLUOROSULFONATE IONOMER MEMBRANES

Bing Yan

Thesis submitted to the faculty of the Virginia Polytechnic Institute and State University in partial fulfillment of the requirements for the degree of

Master of Science
In
Chemistry

Robert B. Moore, chair
Louis A. Madsen
Hervé Marand

July 27, 2010
Blacksburg, Virginia

Keywords: Keywords: perfluorosulfonate ionomers, Nafion®, morphology, crystallinity, thermal treatment

EFFECTS OF THERMAL TREATMENTS ON PERFLUOROSULFONATE IONOMER MEMBRANES

Bing Yan

ABSTRACT

Perfluorosulfonate ionomer (PFSI) membranes were annealed at elevated temperature for various periods of time in order to investigate the morphological effects of thermal treatments. For Nafion® 117, the DSC thermograms of Na^+-, Cs^+- and tetramethylammonium(TMA^+)-form membranes show an endothermic peak develops upon annealing at 200°C, indicating the development of crystallinity in the membrane. For these three samples annealed under same conditions, the heat of fusion (ΔH) values of the endothermic event increases with increasing counterion size. Larger tetraalkylammonium ions, tetraethylammonium(TEA^+) and tetrapropylammonium(TPA^+), result in no significant peak upon annealing at 200°C. DSC thermograms of annealed Na^+-form 3M Ionomer show no peak upon annealing and DSC thermograms of annealed TMA^+-form 3M Ionomer show a very small peak that develops with annealing time at high equivalent weights. Annealed TMA^+-form Dow Ionomer, which has a side chain shorter than both Nafion® and 3M Ionomer and a smaller mole% of side chains at the same equivalent weight, shows a relatively high ΔH value, which might also be related to its blocky nature. These results show that the isothermal crystallization kinetics of PFSI is affected by the counterion attached to the sulfonate group, the length of side chain, the mole% of side chains and the nature of the membrane. Water uptake analysis has been performed on annealed membranes, and the result shows that water uptake decreases with increasing degree of crystallinity.

Acknowledgements

First of all, I wish to thank my research advisor, Dr. Robert B. Moore, for his guidance and encouragement during my graduate study at Virginia Tech. I would also like to thank all past and present members of the Moore research group, Shawn Osborn, Jong Keun Park, Sonya Benson, Gilles Divoux, Angela Osborn, Ninad Dixit, Scott Forbey, Elise Naughton, Katherine Finley, Mingqiang Zhang, Nathan May and Kate Magruder, for their support and assistance throughout the past three years.

I would like to thank my committee members, Drs. Hervé Marand and Louis A. Madsen for the guidance they have provided. I also wish to thank Dr. Paul A. Deck, our director of graduate studies, for his advice, understanding and patience throughout my entire graduate study at Virginia Tech, and the staff members of the chemistry department, especially Carla Slebodnick and Angie Miller for their invaluable assistance.

I also thank the National Science Foundation for supporting this research project.

Finally, I want to thank my parents, Xuemin Yan and Xiaowen Zheng for their unchanging love and support.

Table of Content

List of Figures

List of Tables

1. Fuel Cell Technology and Perfluorosulfonate Ionomers

I. Introduction

A. Fuel Cell Technology

Fuel cells are one of the oldest electrical power generation technologies. Because of their high energy efficiencies and low pollution generation, fuel cells may be excellent options for future energy sources.[1] During the past decade there have been remarkable developments in fuel cell technology, but there still are obstacles to overcome before fuel cells can be widely used as a power source. These obstacles include, but are not limited to, performance, cost, operating conditions and long-term durability.

1) Historical Perspective of Fuel Cells

The invention of fuel cells as an electrical energy conversion method was made in 1839 by an Englishman named Sir William Grove,[2] and the principle was discovered by Christian Friedrich Schönbein, a professor at the University of Basle.[1] Although the discovery of the fuel cell was well before the invention of the internal combustion engine (ICE), its development has lagged behind the development of the ICE, partially due to the fact that during the first century after the invention of fuel cells, nonrenewable energy sources were abundant and environmental consequences of fossil fuel use did not draw much attention.

The concept of fuel cell was revived in the 1930's by Francis T. Bacon. In 1959, powering a forklift truck with a power output of 5 kW, he presented his Alkaline Fuel Cell demonstration, which used a KOH electrolyte and oxygen and hydrogen as fuels.[2,3]

Also in 1959, Willard Grubb received a U.S. patent for his design of a fuel cell, which is the first design containing an ion-exchange resin as the electrolyte.[3] This ion-exchange resin was copolymerized from m-phenolsulfonic acid and formaldehyde, and allowed cations to permeate through the membrane, while electrons had to travel through the circuit outside the cell. Grubb was the first to show that a fuel cell contains a three-phase interface between the reactants, the electrolyte, and catalyst in the electrode. The term "proton exchange membrane fuel cell" (PEMFC) was used for fuel cells that use ion-exchange resins as electrolytes.

The first successful practical applications of fuel cells were in space technologies. In the NASA Apollo Space Program from 1960 to 1965, the alkaline fuel cell system was used.[4] This is also considered by some to be the start of a new era for fuel cells. In 1992 the first zero-emission bus powered only by PEMFCs was made by Ballard Power Systems.[3] During the past few decades, many research groups began to focus on fuel cells and their application.

2) Types of Fuel Cells

a. Alkaline Fuel Cell (AFC)

The alkaline fuel cell (Figure 1.1) is a low temperature fuel cell whose operating temperature is usually below 100 ºC.[1] In AFC, the oxidation and reduction reactions occur in alkaline media, and OH^- acts as the charge carrier in the electrolyte. OH- ions are formed in the reduction of water, and travel through the electrolyte to the anode, where they combine with hydrogen and form water in the oxidation reaction. Equations 1-1 - 1-3 show the electrochemical reactions taking place at the cathode, the anode, and in the overall cell.

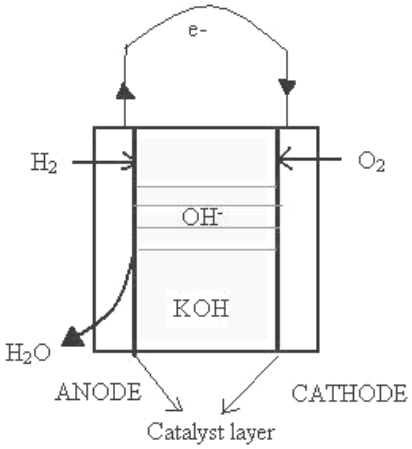

Figure 1.1 Alkaline fuel cell

Cathode: ½ $O_2(g) + H_2O(l) + 2e^- \rightarrow 2OH^-(aq)$ 1-1

Anode: $H_2(g) + 2OH^-(aq) \rightarrow 2H_2O(l) + 2e^-$ 1-2

Overall: $H_2(g) + ½ O_2(g) \rightarrow H_2O(l)$ 1-3

The oxygen reduction kinetics in alkaline electrolyte is usually much faster than in acidic fuel cells, which makes the AFC more efficient.[1,4] However, the hydrogen oxidation reaction in alkaline electrolyte is slower than in acid. The main disadvantage of AFC is that it only works well when very pure gases are used,[1,4] which strongly restricts the application of AFC.

b. Phosphoric Acid Fuel Cell (PAFC)

The operating temperature of PAFC (Figure 1.2) is between 160 ºC and 220 ºC. The PAFC, as for now, is the most developed fuel cell system in term of commercial applications. The PAFCs are usually used in stationary power plants with outputs ranging from 0.2 to 20 MW[1,4].

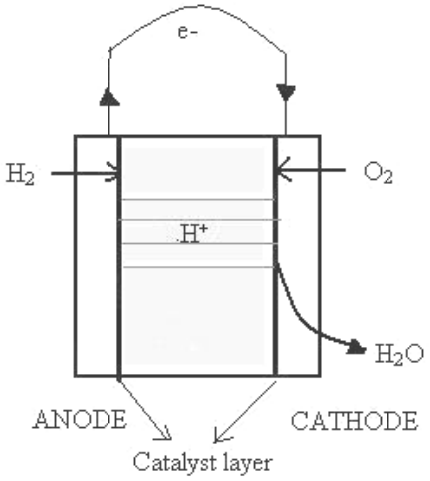

Figure 1.2 Phosphoric acid fuel cell

The cathode, anode and overall reactions taking place in the PAFC are shown in Equations 1-4 – 1-6:

Cathode: $\frac{1}{2} O_2(g) + 2H^+(aq) + 2e^- \rightarrow H_2O(g)$ 1-4

Anode: $H_2(g) \rightarrow 2H^+(aq) + 2e^-$ 1-5

Overall: $\frac{1}{2} O_2(g) + H_2(g) \rightarrow H_2O(g)$ 1-6

The main advantages of PAFC, besides its simple construction, include its thermal, chemical and electrochemical stability and low electrolyte volatility at the operation temperature. Because of these advantages, PAFC has received great commercial development.[4,5]

c. Proton Exchange Membrane Fuel Cell (PEMFC)

Proton exchange membrane fuel cells (Figure 1.3) are also low-temperature fuel cells, with operating temperatures generally lying between 85 ºC and 105 ºC. This type of fuel cell uses

proton exchange membranes as electrolytes and therefore is also called solid polymer electrolyte fuel cells (SPEFC).

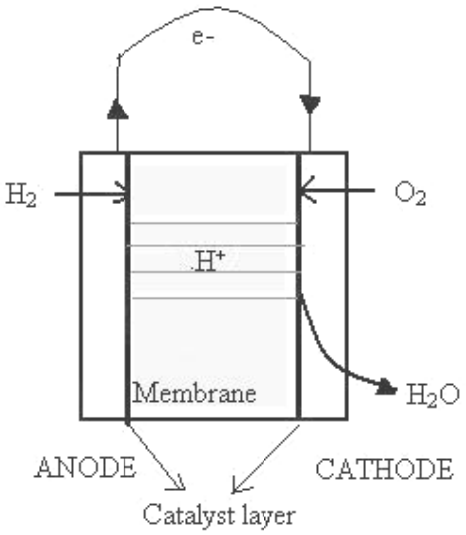

Figure 1.3 Proton exchange membrane fuel cell

The cathode, anode and overall reactions in PEMFC, shown in Equations 1-7 -1-9, are the same as in PAFC. In PEMFC, hydrogen is oxidized in the anode reaction. The protons formed then travel through the polymer membrane to the cathode. At the cathode oxygen reduction occurs and water is formed.

Cathode: $\frac{1}{2}\ O_2(g) + 2H^+(aq) + 2e^- \rightarrow H_2O(l)$ 1-7

Anode: $H_2(g) \rightarrow 2H^+(aq) + 2e^-$ 1-8

Overall: $\frac{1}{2}\ O_2(g) + H_2(g) \rightarrow H_2O(l)$ 1-9

The assembly of the electrolyte and electrodes is usually called a membrane electrode assembly or an MEA.[6,7] An MEA consists of a membrane, two catalyst layers/electrodes, and

two gas diffusion layers (GDL). The main purpose of having GDLs is to ensure direct and uniform supply of the fuel and oxidant gases to the catalyst layers, where the electrochemical reaction is initiated. The GDL is usually porous carbon paper or cloth coated with polytetrafluoroethylene.[6]

The commonly used catalyst layers are composed of platinum particles in carbon supports. Various studies have involved attempts to enhance the utilization of platinum and increase the tolerance to carbon monoxide poisoning.

The proton exchange membrane is a very important part in PEMFC technology and may well be one of the determining factors for the future application of PEMFCs. This part will be discussed in more details later.

The PEMFCs were the first fuel cells to be used in space technologies. In the early 1960's, the Gemini Space Program used a 1kW fuel cell stack, but NASA later turned to AFC instead of PEMFC for its further projects.[8]

i) Direct Methanol Fuel Cell (DMFC)

The direct methanol fuel cell (Figure 1.4) is a special form of PEMFC. Its operating temperature is generally similar to that of PEMFCs. In a DMFC, methanol is directly used as the fuel. The benefits of this includes that methanol is liquid at operating temperatures, the high specific energy of methanol, and its availability from renewable resources.

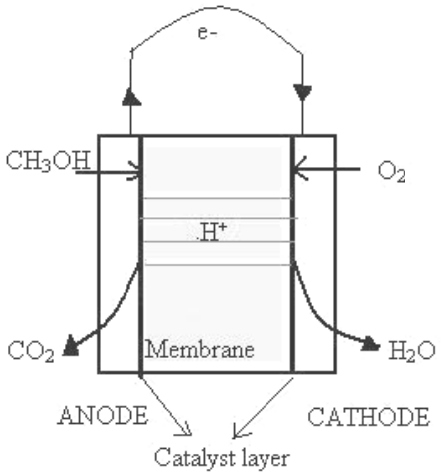

Figure 1.4 Direct methanol fuel cell

The reactions taking place at the cathode, the anode in a DMFC and the overall reaction are shown in Equations 1-10 – 1-12:

Cathode: $3/2\ O_2(g) + 6H^+(g) + 6e^- \rightarrow 3H_2O(g)$ 1-10

Anode: $CH_3OH(l) + H_2O(l) \rightarrow CO_2(g) + 6H^+(aq) + 6e^-$ 1-11

Overall: $CH_3OH(l) + 3/2\ O_2(g) \rightarrow CO_2(g) + 2H_2O(l)$ 1-12

Many membranes used in DMFCs are originally designed for PEM applications with an emphasis on increasing the proton conductivity. However, in DMFCs, methanol can also travel to the cathode because of electroosmotic drag. Methanol can then cause a mixed potential at the cathode due to its own oxidation, which therefore decreases the fuel cell performance. There are several major approaches to deal with the methanol cross-over problem. One is to use membranes that have low permeability of liquid methanol, such as thicker membranes,[9] Cs^+ -

doped membranes, and some alternative membranes. Another way is to find methanol-tolerant catalysts/cathodes.[10-12] Also, because the cross-over effect is dependent on methanol concentration, there is considered to be an optimum concentration of 2M methanol in water.[13,14]

ii) Other Types of PEMFCs

There are other types of fuel cells that are based on PEM technology. Examples include direct ethanol fuel cell (DEFC) and direct formic acid fuel cell (DFAFC). The principles of these fuel cells are similar to that discussed previously.

d. High Temperature Fuel Cells

Besides those low temperature fuel cells mentioned previously, there are also high temperature fuel cells, which have operating temperatures between 500 ºC and 1000 ºC. Two common types of high temperature fuel cells are the Molten Carbonate Fuel Cell (MCFC) and Solid Oxide Fuel Cell (SOFC).

3) Advantages of Fuel Cell Technology

As mentioned before, fuel cells are generally more environmental friendly than traditional power sources. Another significant advantage of fuel cells is their efficiency. In a heat engine (Figure 1.5) that works between a hot reservoir and a cold reservoir, gaining heat from the hot reservoir, converting part of Q_1 to work W and releasing heat Q_2 to the cold reservoir, the maximum efficiency of the system is restricted by the Carnot Efficiency, $\varepsilon^{thermal}$:

$$\varepsilon \leq \varepsilon^{\text{thermal}} = 1 - \frac{T_2}{T_1} \qquad 1\text{-}13$$

in which T_1 and T_2 are the temperatures of the hot and cold reservoir, respectively. In general, the efficiencies of these heat engines are often below 50%.

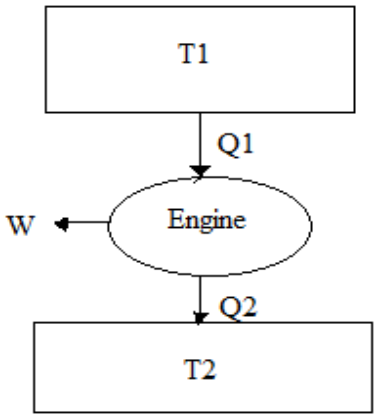

Figure 1.5 Heat engine

In fuel cells, however, the maximum efficiency is not bound by the Carnot Cycle. The maximum efficiency of a fuel cell, ε^{cell}, is given by:

$$\varepsilon^{cell} = \frac{\Delta G}{\Delta H} = 1 - \frac{T\Delta S}{\Delta H} \qquad 1\text{-}14$$

In which ΔG, ΔH and ΔS are the Gibbs free energy, the enthalpy change, and the isothermal entropy change of the fuel cell process, respectively. In reality, there are factors that cause decrease in the efficiencies of fuel cells, such as electrode overpotentials, electrolyte resistance, fuel utilizations, etc. However, in spite of these factors, fuel cells are still superior to heat engines as far as efficiency is considered.

B. Polymer Electrolyte Membranes in PEMFC

1) Chemical and Physical Requirements for Polymer Electrolyte Membranes

The main requirements for polymer electrolyte membranes, besides that they should have high proton conductivity, include mechanical and electrochemical stability. The fuel cell

membrane used in the Gemini Space Program was a polystyrene sulfonate (PSS) polymer membrane, which turned out to have limited lifetime due to the lack of chemical stability. This was one of the reasons that caused NASA to use AFC instead of PEMFC for its other programs.

Thermal stability is another important property of proton exchange membranes. In a reversible cell, the Gibbs free energy of the electrochemical reaction is:

$$\Delta G = \Delta G^0 + RT \ln J \qquad 1\text{-}15$$

$$J = \prod_B a_B{}^{\nu_B} \qquad 1\text{-}16$$

in which ΔG^0 is the Gibbs free energy of the reaction at the standard state, R is the universal gas constant, T is the temperature, a_B and ν_B are the activity and stoichiometric coefficient, respectively. Since

$$\Delta G = -nFE,\ \Delta G^0 = -nFE^0 \qquad 1\text{-}17$$

in which n is the number of electrons in the reduction or oxidation reaction, the potential can therefore be written as

$$E = E^0 - \frac{RT}{nF} \ln J \qquad 1\text{-}18$$

which is the Nernst Equation and can be used to demonstrate the ideal performance of a fuel cell:

$$E = E^o + (RT/2F)\ln[P_{H2}/P_{H2O}] + (RT/2F)\ln[\sqrt{P_{O2}}] \qquad 1\text{-}19$$

In which P_{H2}, P_{H2O} and P_{O2} are the partial pressures of each gas, respectively.

As can be seen from Equation 1-19, the ideal fuel cell potential is dependent on temperature and pressures. Therefore, operating at a higher temperature can increase the ideal cell potential.

However, since the proton exchange membrane is temperature-sensitive, it may limit the operating temperature of the fuel cell.

2) Nafion® and Other Perfluorosulfonate Membranes

a. Structure

The use of Nafion® membranes is considered to be a major breakthrough in the development of PEMFCs. Nafion® is an ionomer first created in the 1960s by DuPont[15]. It is generally prepared by copolymerizing a perfuorinated vinyl ether comonomer with tetrafluoroethylene (TFE)[16]. It is perhaps the most studied membrane material in PEMFCs and is considered the benchmark polymer used in PEMFCs.

The chemical structure of Nafion® is shown below (Figure 1.6), where n varies with different equivalent weight, which is defined as the grams of polymer per mole of sulfonic acid groups:

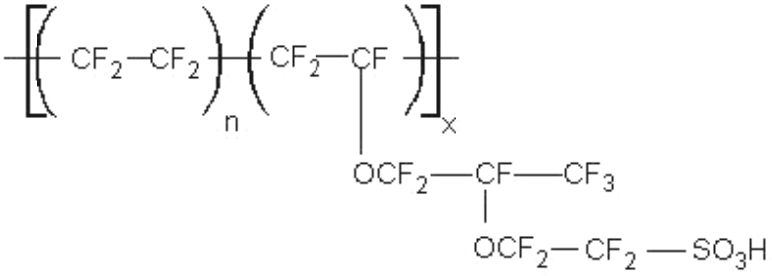

Figure 1.6 Chemical structure of Nafion®

Because the molar weights of tetrafluoroethylene and the comonomer are 100 g/mol and 443 g/mol, respectively, the equivalent weight of Nafion®, which is defined as the number of grams of polymer per equivalent of sulfonic acid, can then be expressed as EW = 100 (n) + 443.[17] The most commonly seen equivalent weight of Nafion® is 1100.

b. Chemical and Mechanical Properties

The tetrafluoroethylene backbone in Nafion® is chemically inert in common reducing and oxidizing environments. This structure also imparts higher stability than hydrocarbon polymers usually have, giving Nafion® a higher operating temperature[18]. The combination of the stable TFE backbone with the sulfonic group gives Nafion® excellent transport properties and mechanical stability[19]. At high ion concentrations, aggregates, which behave as physical crosslinks, are formed, giving higher mechanical strength and providing a percolation pathway for cations[20].

Since there are strong interactions between ionic groups, membrane processing may be difficult. In its thermoplastic sulfonyl fluoride ($-SO_2F$) precursor form, however, Nafion® is processable and can be extruded into films of designed thickness. The films can then be converted to other forms, such as acid form, by boiling in HNO_3 solution; K^+ form, Cs^+ and Na^+ form, by soaking and heating the acid form membrane in base solutions; and tetra-alkylammonium forms, by soaking the membrane in solution of tetra-alkylammonium hydroxide overnight.

c. Applications

The applications of Nafion®, other than as proton conductor in PEMFCs, also include as superacid catalyst in organic synthesis[21] and as membranes in chlor-alkali cells[22], where Nafion® acts as a membrane between half cells. It has also been considered to have potential as sensors[23].

3) Alternative Membranes

Although Nafion® is still the standard membrane for PEMFC applications, there are other alternative membranes under investigation. Dow Chemical introduced a perfluorinated ionomer

that has a much shorter side chain[24]. This ionomer, now called the Hyflon Ion, has become a product of Solvay Solexis[25]. The chemical structure of the Hyflon Ion is shown in Figure 1.7. The equivalent weight of the Hyflon Ion is EW = 100 (n) + 277.

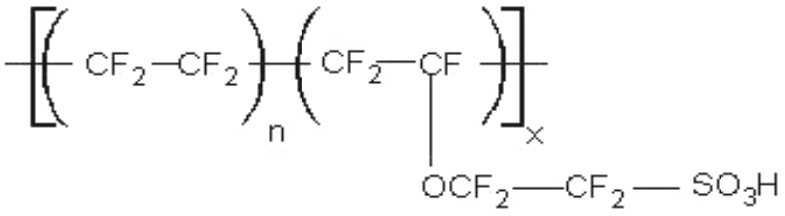

Figure 1.7 Chemical structure of the Hyflon Ion

3M has recently introduced an ionomer[26, 27] that has an intermediate side chain length between Nafion® and the Hyflon Ion. Figure 1.8 shows the chemical structure of the 3M ionomer. The equivalent weight of the 3M ionomer is EW = 100 (n) + 377. Like Nafion®, both the Hyflon Ion and the 3M ionomer can form the "Teflon-like" crystallites.

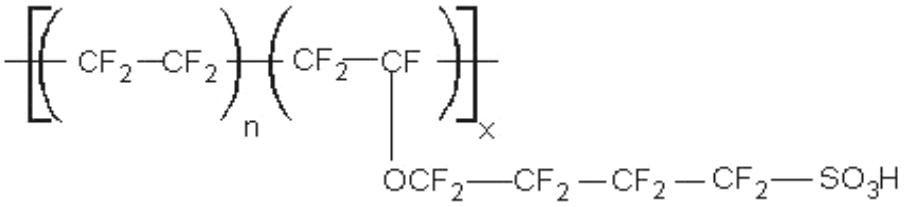

Figure 1.8 Chemical structure of the 3M Ionomer

Hydrated sulfonated polyether ether ketone (sPEEK) has been found to have similar properties as Nafion®[28,29]. Irradiation-grafted PVDF-PS-sulfonic acid, manufactured by grafting polystyrene onto poly(vinylidene fluoride) backbone before being sulfonated, is another type of membrane that can be used in PEM fuel cells[30].

II. Morphological Features of Perfluorosulfonate Ionomers

In perluorosulfonate ionomers, the perfluoroether side chains, which contain the sulfonate groups, organize into aggregates. This leads to a complex multi-phase morphology, in which the ionic domains, termed clusters, are distributed throughout the polytetrafluoroethylene matrix, while segments of the tetrafluoroethylene backbone are capable of organizing into poly(tetrafluoroethene)-like crystalline domains[17,31].

A. Models for the Morphology of Nafion®

1) Historic Perspective

Since the morphology of Nafion® is very complex, during the past three decades, numerous investigations have been made in order to find a model that can successfully describe the morphology of this kind of ionomers.

Before those various models of Nafion® were developed, Eisenberg and Yeo proposed a theory for ionomers in general. In this theory, at low ion concentration, the ions form "multiplets", an aggregate containing only ionic material[32]. This led to the Multiplet-Cluster model for ionomers, in which the multiplet formation is largely dependent on the electrostatic interactions between the ion pairs[33]. At high ion concentration, the more extensive aggregation leads to the formation of clusters that contain both ionic material and a considerable portion of organic polymer[32].

The Eisenberg-Hird-Moore (EHM) Model[33], proposed in 1990, is based on the existence of the ionic aggregates. A novel feature of this model is the restriction of chain mobility in regions surrounding the multiplets. The thickness of the region of reduced mobility is expected to be of the order of the persistence length of the polymer chain. A lone multiplet, acting as a crosslink, is

expected to increase the glass transition temperature of the material. However, the total size of the multiplet plus the region of restricted mobility is not large enough to have its own T_g. As the concentration of the ionic groups gets higher, regions of restricted mobility will overlap and larger, contiguous region of restricted mobility will be formed. When the region is large enough, it will have its own T_g and become a cluster. The clusters exhibit phase-separated behavior and have much higher T_g. The schematic representation of the multiplet and the region of reduced mobility is shown in Figure 1.9.

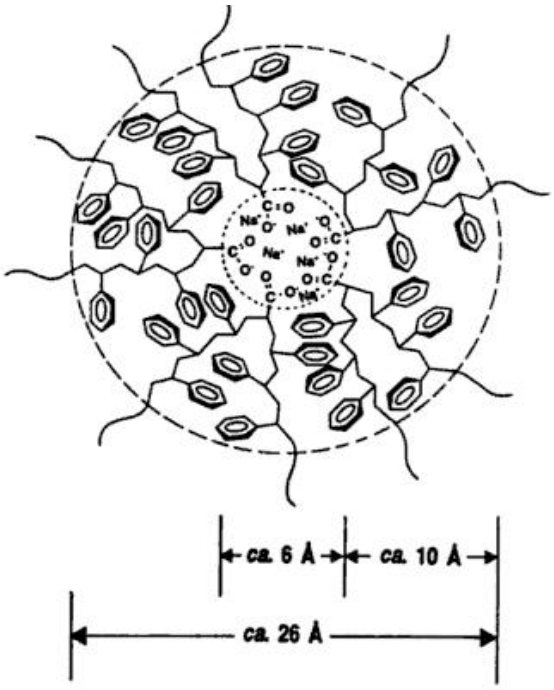

Figure 1.9 The schematic representation of the multiplet and the region of reduced mobility (reprinted with permission from ref. 33. Copyright 1990, American Chemical Society)

A historical model that has been widely refrenced is the model for the water-swollen morphology of Nafion® proposed by Gierke and co-workers in the early 1980s, based on small

angle x-ray scattering (SAXS) data[19,34]. In this model, upon water swelling, the ionomer was portrayed as a composition of spherical ionic clusters with an inverted micelle structure interconnected by ionic-lined channels, forming the morphology referred to as the cluster-network model (Figure 1.10) [34]. The narrow channels between swollen clusters can form a percolation pathway which allows ionic transport. The membrane is cation selective because the anionic sites repel each other. The permselectivity of Nafion® can persist beyond the Donnan limit and is called "superselective".

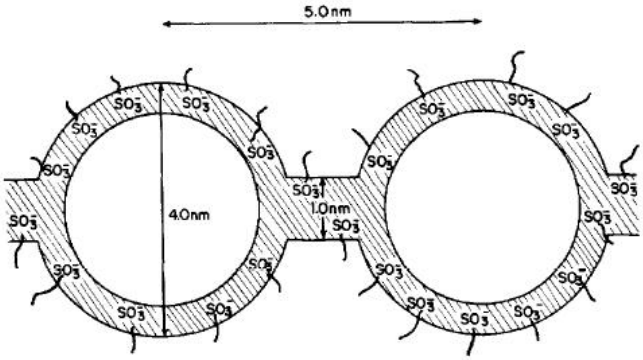

Figure 1.10 Cluster-network model of Nafion® (reprinted with permission from ref. 34. Copyright 1983, Elsevier)

2) Current Understanding

Some current model for the morphology of Nafion® include a lamellar model proposed by Litt[35], a rod-like model proposed by Rubatat and co-workers[36], and a fringed-micelle model proposed by Kim et al[37]. Figure 1.11 shows schematic representations of these models. A recently proposed parallel water-channel model by Schmidt-Rohr[38] is shown in Figure 1.12.

The lamellar model is based on the theory that longer crystallizable sequences will chain fold to an average lamellar thickness. The lamella form a micelle with the surface lined with

ionic groups and the interior composed of noncrystalline tie chains[35]. Rubatat's rod-like model suggests extended chain crystals that are distributed in the rods[36]. The parallel water-channel model suggests that the ionic side group lining the water channel while with the backbone forming the cylinder wall[38]. In the fringed-micelle model proposed by Kim et al, the crystallites are distributed randomly in the perfluorinated matrix[37].

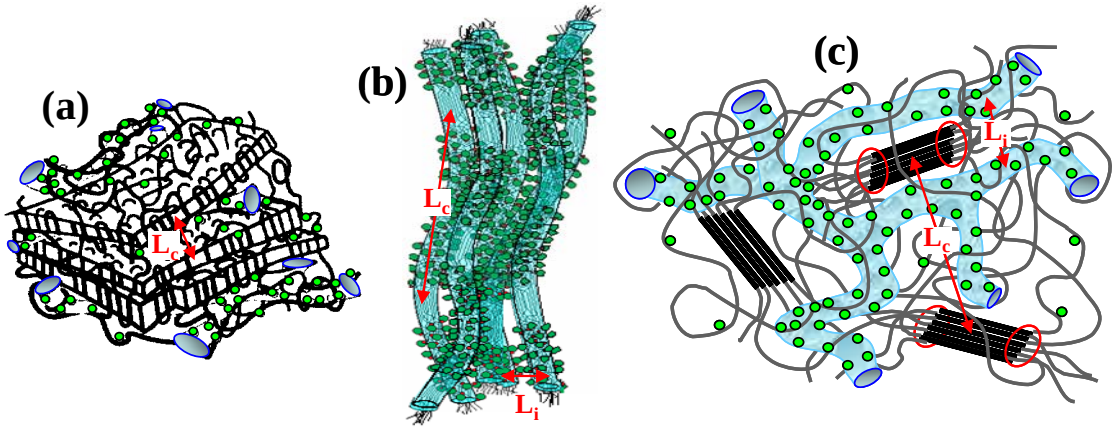

Figure 1.11 Schematic representations of (a) lamellar model; (b) rod-like model; and (c) fringed-micelle model

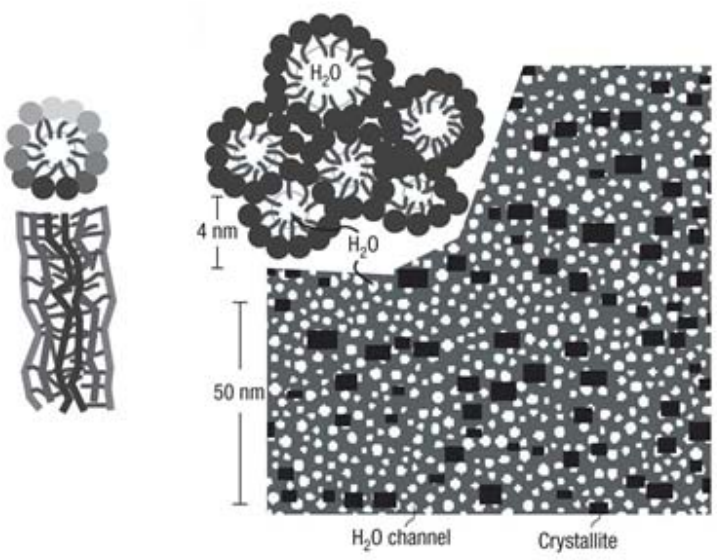

Figure 1.12 Schematic representation of parallel water-channel model (reprinted with permission from ref. 38. Copyright 2008, Nature Publishing Group)

All these models recognize the formation of a connected network of ionic aggregates in the polytetrafluoroethylene matrix, which allows swelling and proton transport. However, these models have significant differences with respect to the spatial distribution of the crystalline structures. These differences also suggest different roles of the crystallites in affecting membrane properties. To clearly address the structure of the crystalline component in perfluorosulfonate ionomers and the effect crystallites have on membrane properties, further work is needed.

B. The Crystalline Domains

Gierke et al examined the morphological features of Nafion® with different equivalent weights ranging from 1100 to 1800 using wide-angle x-ray diffraction (WAXD) and SAXS[19,39]. Their WAXD results showed for the unhydrolyzed precursor a crystalline peak at 18º, 2θ was observed with an intensity increasing with equivalent weight. The degree of crystallinity was estimated to range between 0 and 40wt% by comparing the crystalline peak with the relative

intensity of the amorphous halo. For hydrolyzed Nafion®, a low angle SAXS maximum at ca. 0.5º, 2θ, a broad peak halo at ca. 1.6º, 2θ and a peak at 18º, 2θ were observed. The WAXD data showed a decrease in crystallinity compared to the precursor. They also concluded that unlike poly(tetrafluoroethylene), the melting of Nafion® occurs over a broader temperature range due to the crystallites' broader size range.

Fujimura et al. [40,41] reported the intensity of the low angle maximum increases with increasing equivalent weight, and attributed the low angle scattering maximum to an average spacing between crystalline lamellar platelets based on SAXS and WAXD information as well as the behavior observed with uniaxial deformation.

By using x-ray diffraction analysis of oriented fiber samples, Starkweather further studied the crystallites in Nafion®. The results indicated that the crystallites were packed in a hexagonal lattice with cell dimensions similar to that of PTFE[17].

Gebel and Moore[42] studied short side-chain PFSIs and found the swelling behavior of the ionic domain to be identical to that of Nafion®, while the interlamellar spacings shift in a different way with water content from that of the inter-cluster spacings. These results indicate that the lamellar model proposed by Litt[35] is an over-simplification of the morphology of Nafion®.

Moore and Martin[31] studied the effects of solvents and temperature on the crystallinity using differential scanning calorimetry (DSC). The two peaks at 140 ºC and 240 ºC were thought to be the Tg of the matrix and the Tg of the ionic clusters, respectively. Today, it is believed that the peak at 240 ºC is due to the melting of the PTFE-like crystallites, and that the peak at 140 ºC

is due to the melting of small imperfect crystallites that are formed in "thermal equilibrium" with the annealing temperature[43].

C. Methods of Controlling the Degree and Organization of Crystallinity in Perfluorosulfonate Ionomers

There are various methods to control the degree and organization of crystallinity in PFSIs, including thermal treatment[43], solution and melt-processing[32,44-46], and mechanical orientation[47]. Heating Nafion® at 330 ºC can eliminate crystallinity and standard crystallization procedures like isothermal crystallization can be used to produce samples with different degrees of crystallinity. Solution and melt-processing parameters such as temperature, time and couterion types can be adjusted in order to obtain controlled degrees of crystallinity. There are reports demonstrating that oriented PFSI membranes have shown some special properties and behaviors. For example, Mauritz and Moore reported that uniaxial orientation results in anisotropic ionic conductivity[48]

References

1. Carrette, L.; Friedrich, K. A.; Stimming, U. *Fuel Cells* **2001,** *1*, 5-39.
2. Bacon, F. T. *Electrochimica Acta* **1969,** *14*, 569-585.
3. Stone, C.; Morrison, A. E. *Solid State Ionics* **2002,** *152-153*, 1-13.
4. Carrette, L.; Friedrich, K. A.; Stimming, U. *Chemphyschem* **2000,** *1*, 162-193.
5. Brenscheidt, T.; Janowitz, K.; Salge, H. J.; Wendt, H.; Brammer, F. *Int. J. Hydrog. Energy* **1998,** *23*, 53-56.
6. Ma, C.; Zhang, L.; Mukerjee, S.; Ofer, D.; Nair, B. *J Membrane Sci* **2003,** *219* (1-2), 123-136.
7. Mehta, V.; Cooper, J. S. *Journal of Power Sources* **2003,** *114*, 32-53.
8. Wright, P. V. *Electrochimica Acta* **1998,** *43*, 1137-1143.

9. Ren, X.; Springer, T. E.; Gottesfeld, S. *Journal of The Electrochemical Society* **2000,** *147*, 92-98.
10. Alonso-Vante, N.; Tributsch, H.; Solorza-Feria, O. *Electrochimica Acta* **1995,** *40*, 567-576.
11. Solorza-Feria, O.; Ellmer, K.; Giersig, M.; Alonso-Vante, N. *Electrochimica Acta* **1994,** *39*, 1647-1653.
12. Gupta, S.; Tryk, D.; Zecevic, S. K.; Aldred, W.; Guo, D.; Savinell, R. F. *J. Appl. Electrochem.* **1998,** *28*, 673-682.
13. Kuver, A.; Vielstich, W. *Journal of Power Sources* **1998,** *74*, 211-218.
14. Ravikumar, M. K.; Shukla, A. K. *Journal of The Electrochemical Society* **1996,** *143*, 2601-2606.
15. Connolly, D. A.; Gresham, W. F., Fluorocarbon Vinyl Ether Polymers. Patent US3282875, **1966**.
16. Mauritz, K. A.; Moore, R. B. *Chem. Rev.* **2004,** *104*, 4535-4585.
17. Starkweather, H. W. *Macromolecules* **1982,** *15*, 320-323.
18. Curtin, D. E.; Lousenberg, R. D.; Henry, T. J.; Tangeman, P. C.; Tisack, M. E. *Journal of Power Sources* **2004,** *131*, 41-48.
19. Gierke, T. D.; Munn, G. E.; Wilson, F. C. *J. Polym. Sci. Pt. B-Polym. Phys.* **1981,** *19*, 1687-1704.
20. Gebel, G.; Lambard, J. *Macromolecules* **1997,** *30*, 7914-7920.
21. Doyle, M. R., G., *Handbook of Fuel Cells - Fundamentals, Technology and Applications*. John Wiley & Sons: Chichester, 2003; Vol. 3, p 351-395.

22. Gavach, C. P., G., *Proton Conductors Solids, Membranes and Gels - Materials and Devices*. Cambridge University Press: Cambridge, 1992; p 487-498.

23. HeitnerWirguin, C. *J Membrane Sci* **1996,** *120*, 1-33.

24. Ezzell, B. R.; Carl, W. P.; Mod, W. A., Novel polymer having acid functionality. Patent US4330654, **1982**.

25. Arcella, V.; Ghielmi, A.; Apostolo, M.; Abusleme, J., Fluorinated ionomers. European Patent Application 01114606.5, **2001**.

26. Guerra, M. A. Preparation of perfluorinated vinyl ethers having a sulfonyl fluoride end-group. Patent US6624328, **2003**.

27. Hamrock, S. J.; Rivard, L. M.; Innes Moore, G. G.; Freemyer, H. T., Polymer electrolyte membrane. Patent Application US29949121219, **2004**.

28. Kreuer, K. D. *J Membrane Sci* **2001,** *185*, 29-39.

29. Alberti, G.; Casciola, M. *Solid State Ionics* **2001,** *145,* 3-16.

30. Norby, T. *Solid State Ionics* **1999,** *125*, 1-11.

31. Moore, R. B.; Martin, C. R. *Macromolecules* **1988,** *21*, 1334-1339.

32. Yeo, S. C.; Eisenberg, A. *J. Appl. Polym. Sci.* **1977,** *21*, 875-898.

33. Eisenberg, A.; Hird, B.; Moore, R. B. *Macromolecules* **1990,** *23*, 4098-4107.

34. Hsu, W. Y.; Gierke, T. D. *J Membrane Sci* **1983,** *13*, 307-326.

35. Litt, M. H. *Polymer Preprints* **1997,** *38*, 80-81.

36. Rubatat, L.; Rollet, A. L.; Gebel, G.; Diat, O. *Macromolecules* **2002,** *35*, 4050-4055.

37. Kim, M. H.; Glinka, C. J.; Grot, S. A.; Grot, W. G. *Macromolecules* **2006,** *39*, 4775-4787.

38. Schmidt-Rohr, K.; Chen, Q. *Nat. Mater.* **2008,** *7* , 75-83.

39. Hsu, W. Y.; Gierke, T. D. *Macromolecules* **1982,** *15*, 101-105.

40. Fujimura, M.; Hashimoto, T.; Kawai, H. *Macromolecules* **1981,** *14*, 1309-1315.

41. Fujimura, M.; Hashimoto, T.; Kawai, H. *Macromolecules* **1982,** *15*, 136-144.

42. Gebel, G.; Moore, R. B. *Macromolecules* **2000,** *33*, 4850-4855.

43. Page, K. A.; Cable, K. M.; Moore, R. B. *Macromolecules* **2005,** *38*, 6472-6484.

44. Moore, R. B.; Martin, C. R. *Anal. Chem.* **1986,** *58*, 2569-2570.

45. Moore, R. B.; Cable, K. M.; Croley, T. L. *J Membrane Sci* **1992,** *75*, 7-14.

46. Phillips, A. K.; Moore, R. B. *J. Polym. Sci. Pt. B-Polym. Phys.* **2006,** *44*, 2267-2277.

47. Page, K. A.; Landis, F. A.; Phillips, A. K.; Moore, R. B. *Macromolecules* **2006,** *39*, 3939-3946.

48. Cable, K. M.; Maurtiz, K. A.; Moore, R. B. *Chem. Mat.* **1995,** *7*, 1601-1603.

2. Sample Preparation

I. Materials

Nafion® 117 CS membranes (1100 g/mol SO_3^- equivalent weight, sulfonic acid form) were obtained from E. I. du Pont de Nemours and Company. 3M ionomers with different equivalent weights (700, 800, 900, 1000, and 1100EW) were obtained from 3M Corporation. According to 3M, these membranes with a thickness of about 25 microns were cast onto 0.002 inch thick Kapton polymide. The 700, 900, 1000 and 1100EW samples were cast out of n-propanol, while the 800EW sample was cast out of methanol and dried under slightly different conditions. Old Dow polymer samples with different equivalent weights (606, 793 and 1040EW) were obtained from Dow Chemical Company in the past. Sodium hydroxide (NaOH) pellets were obtained from VWR International, LLC. and used without further purification. Tetramethylammonium hydroxide (TMAOH), 1.0M aqueous solution was obtained from Alfa Aesar and used without further purification. 50wt% cesium hydroxide (CsOH) solution in water, 20wt% tetraethylammonium hydroxide (TEAOH) solution in water and 1.0M tetrapropylammonium hydroxide (TPAOH) solution in water were obtained from Sigma-Aldrich Co. and used without further purification.

II. Preparation of Membranes

The membranes were boiled in 8M nitric acid (HNO_3) solution under reflux for two hours in order to remove impurities. The membranes were then rinsed in deionized water three times and boiled in deionized water for another hour. After cleaning the membranes were dried in vacuum oven at 70°C overnight.

III. Counterion Exchange

A. Alkali Metal Counterions

The cleaned membranes were stirred in 1.0M aqueous solution of either sodium hydroxide (NaOH) or cesium hydroxide (CsOH) for 12 hours and then boiled in the same solution under reflux for an additional hour. The Nafion® membranes were then rinsed in deionized water three times and boiled in deionized water for another hour. Membranes were dried in vacuum oven at 70°C overnight.

B. Tetraalkylammonium Counterions

The cleaned H^+-form membranes were stirred in excess tetramethylammonium hydroxide (TMAOH), tetraethylammonium hydroxide (TEAOH) or tetrapropylammonium hydroxide (TPAOH) solution for 24 hours. The membranes were then rinsed in methanol three times and stirred in methanol for 12 hours before they were dried in vacuum oven at 70°C overnight.

IV. Thermal Treatments

Membranes were heated at 330°C for three minutes to erase previous history of the samples. The membranes were then annealed at 200°C for various periods of time ranging from 5 minutes to 2 days.

3. Thermal Treatments of Nafion® Membranes in Different Counterion Forms

I. Introduction

The concepts of primary and secondary crystallization are often referred in studies on polymer systems. The primary crystallization, which is the fast increase of crystallinity during the early stage of crystallization, is considered to be related to the development of lamellae from the unconstraint melt state. The secondary crystallization is the further increase in crystallinity through crystallization in the melt constrained by the lamellae formed during primary crystallization. Marand et al.[1,2] proposed a model that relates the secondary crystallization mechanism with the crystallization condition and the nature of the polymer chains. It is suggested that secondary crystals are formed at low temperatures, while lamellae thickening happens at temperatures above a certain critical value.

A copolymer such as PFSI can be considered as containing crystallizable units and uncrystallizalbe units that act as defects. Assuming that the defects are excluded from the crystallites and based on phase equilibrium assumption, Flory[3] proposed a theory that relates the melting temperature with the crystallizable sequence length distribution. In this theory, only sequences that exceed a certain length value can crystallize, while smaller sequences remain in the amorphous domain. Based on their study on random ethylene/1-octene copolymer, Alizadeh et al.[4] showed that the degree of crystallinity is dependent on the branch content. At low temperatures, though, a small change in sequence distribution does not have a significant effect on the degree of crystallinity[5]. On the other hand, Sanchez and Eby[6] proposed a model that assumes that the comonomer can be incorporated into the crystallites and the extent of incorporation is dependent on crystallization temperature. Experimental results[4,5] suggest that only systems with small comonomer size can be successfully described using this model. These

previous studies on copolymer systems can be used as a base for understanding the crystallization and melting behavior of PFSI membranes, which differs from these systems because of the existence of the ionic domain.

A paper by Gierke et al.[7] in 1981 was one of the early reports concerning the effects of annealing Nafion®. Based on WAXD, SAXS and DSC results of unhydrolyzed sulfonyl fluoride form (-SO_2F) Nafion® at various equivalent weights ranging from 1100 to 1800, all of which indicated the disappearance of crystallites at high temperatures, it was suggested that crystallites in Nafion® precursor melt over a broad range and has a melting point of about 275°C. After the sample was hydrolyzed, an additional scattering peak at about 1.6° 2θ, attributed to the existence of ionic clusters, was observed.

Similar results were also noticed by Fujimura et al.[8] in H^+- and Cs^+- forms of Nafion® with different equivalent weights ranging from 1100 to 1500. WAXD results showed that in both forms, the crystalline reflection at 18° 2θ disappeared after annealing at 275°C. The crystalline peak reappear upon cooling, indicating the recrytallization of Nafion®. The authors also suggested that the melting point is lower than that of polytetrafluoroethylene, which is around 330°C, because the side chains inhibit crystallization.

Gebel and coworkers[9] dissolved Li^+-form extruded Nafion® (1100EW) under high temperature and pressure in a mixture of water and ethanol. The "reconstructed" membrane was cast from a high boiling point solvent (*N*-methylformamide (NMF)) at 80°C. WAXD results of this membrane showed no crystalline reflection of Nafion® at 18° 2θ, suggesting the membrane was totally amorphous. The crystalline peak reappeared upon annealing at 150°C for three hours and became more intense with increasing annealing temperature. When annealed at 200°C for

three hours, the membrane showed a crystalline peak with a higher intensity than that of the as-received, extruded Nafion® membrane. SAXS results showed the crystalline peak that shifted to lower q values when the annealing temperature was increased. According to the authors, thermal annealing results in an increase in the size of the lamellar crystallites and makes the development of long-range order in the film possible.

Roche et al.[10] heated Na^+-form Nafion® (1200EW) at 330°C and the disappearance of the intercrystalline peak at around 0.04 $Å^{-1}$ was noticed in the small angle neutron scattering (SANS) result, suggesting the elimination of crystallinity. Lee et al.[11] were able to eliminate the crystalline reflection at 18° 2θ in their WAXD results by heating Nafion® 117 at 300°C in a preheated oven and then quickly quenching the membrane in liquid nitrogen.

Page, Cable and Moore[12] heated Na^+- and Cs^+- forms of extruded Nafion® 117 at 330°C for five minutes and then quenched the membranes back to room temperature. Based on DSC results, the broad endotherm between 200 and 250°C that was present in the as-received membranes before thermal treatments disappeared after heating at 330°C. After annealing the quenched membranes at 200°C for different times, an endotherm reappeared and the heat of fusion (ΔH) value of the endotherm increased with increasing annealing time until it reached a plateau after extended period of time. For the Na^+-form Nafion®, the plateau value of ΔH after annealing at 200°C for 24 hours was 2.7J/g, which is about half of the ΔH value (5J/g) of the as-received membrane. For the Na^+-form Nafion®, on the other hand, by annealing the quenched membrane at 200°C for 24 hours, the endotherm had a ΔH of 5.3J/g, which is very close to the ΔH of the as-received membrane. These results showed that the type of counterion can have a significant effect on the crystallization process during thermal annealing.

The purpose of this section is to investigate the effects of thermal treatments on Na^+-, Cs^+-, TMA^+-, TEA^+- and TPA^+-form Nafion® membranes, especially the development of ordering in the membranes during the annealing process.

II. Experimental

DSC analysis was carried out on a TA Instruments Q2000 differential scanning calorimeter. Thermally annealed Na^+-, Cs^+-, TMA^+-, TEA^+- and TPA^+-form Nafion® samples were scanned at a rate of 20°C/min to 350°C.

III. Results and Discussions

A. DSC Results for Alkali Metal-form Nafion® Samples

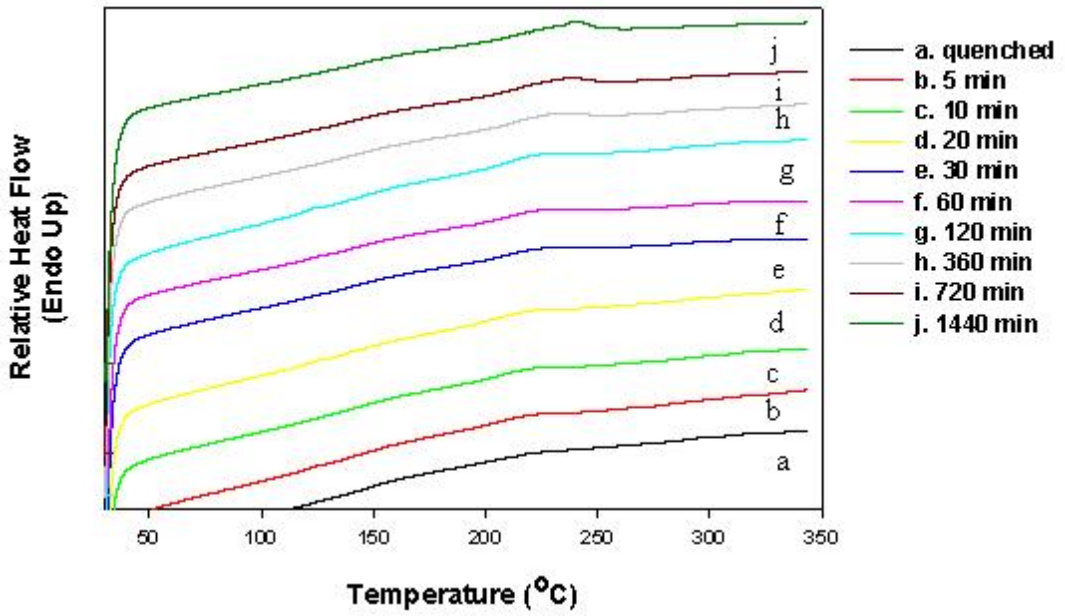

Figure 3.1 DSC thermograms of Na^+-form Nafion® membranes, quenched rescan and annealed at 200°C for various periods of time. For comparison, the thermograms are shifted along the y axis.

Figure 3.1 shows the DSC results for Na^+-form Nafion® membranes after thermal treatments. The DSC curve of the sample quenched after heating at 330°C is virtually flat without any peak. After annealing at 200°C a peak, although not very significant in the graph, appears above the annealing temperature and the magnitude of the endotherm increases with increasing annealing time until it reaches a plateau, showing the development of ordering in the membrane during the thermal annealing. This peak is attributed to the growth of the PTFE-like crystals in the membranes. Similar to previous studies on crystallization of ethylene copolymers, it can also be noticed that the position of the peak maximum shifts to higher temperature when annealed for longer periods of time. Figure 3.2 summarizes the change in the position of the endothermic peak.

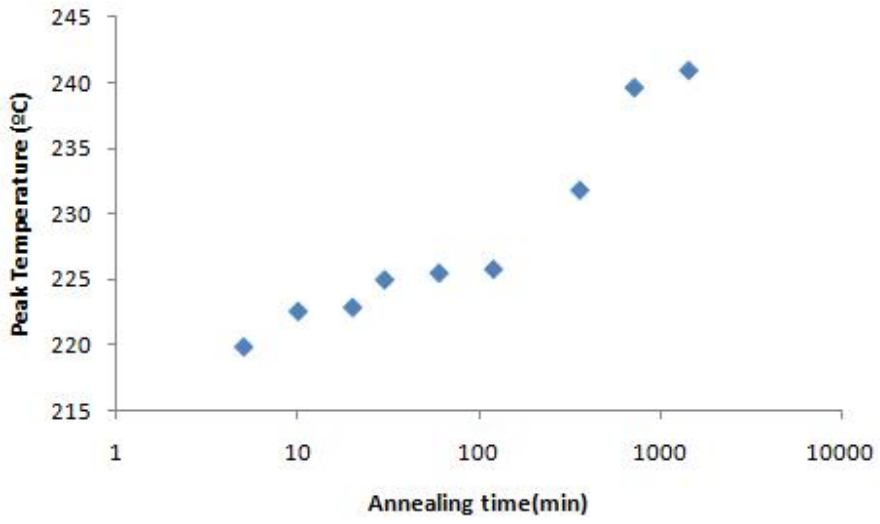

Figure 3.2 Change in peak temperature of Na^+-form Nafion®

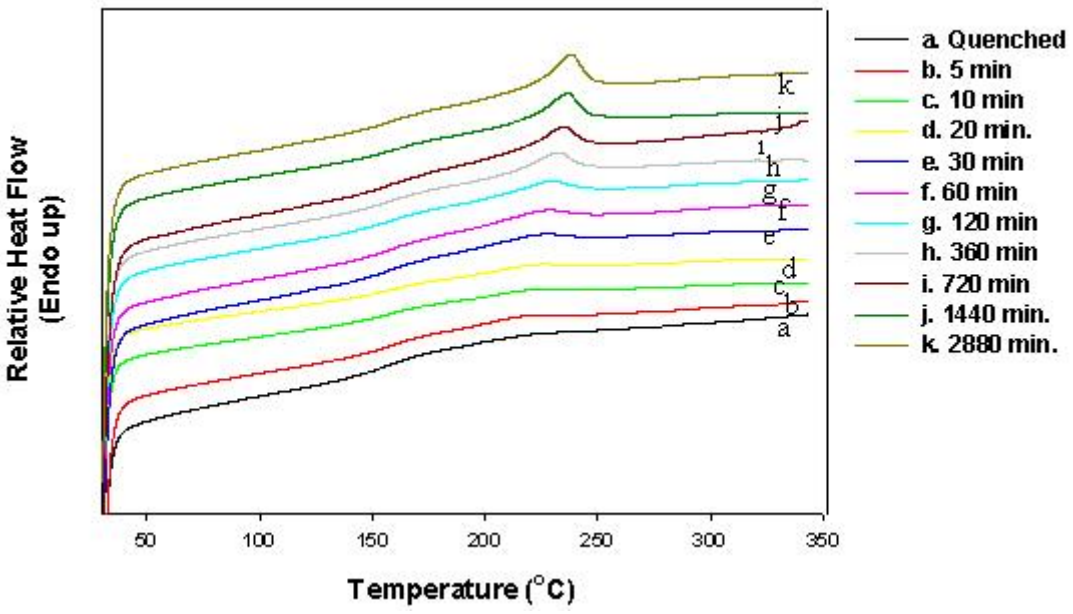

Figure 3.3 DSC thermograms of Cs^+-form Nafion® membranes, quenched rescan and annealed at 200°C for various periods of time. For comparison, the thermograms are shifted along the y axis.

Figure 3.3 shows the DSC results for Cs^+-form Nafion® membranes after thermal treatments. Similarly, a peak grows above the annealing temperature after annealing at 200°C, and the magnitude of the endothermic peak increases as the annealing time increases, showing the development of PTFE-like crystals during the thermal annealing process. Compared to Na^+-form Nafion® membranes, Cs^+-form Nafion® membranes show a more obvious peak in the DCS thermograms. The position of the peak maximum, as summarized in Figure 3.4, also shifts to higher temperature with increasing annealing time. Similar to that observed with the low endotherm in other copolymers[4], the peak temperature and the logarithm of annealing time exhibit a linear relationship.

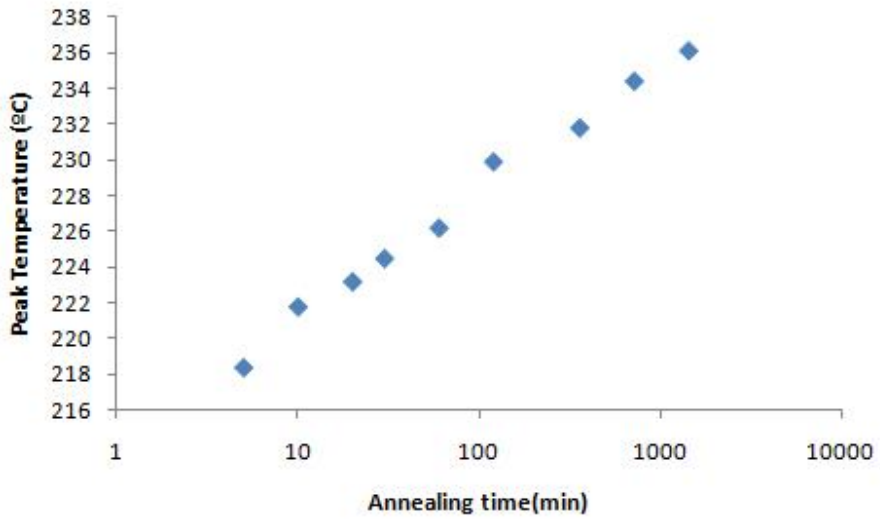

Figure 3.4 Change in peak temperature of Cs^+-form Nafion®

The heat of fusion, ΔH, of the endothermic event can be calculated by integration. The results are showed in Figure 3.5.

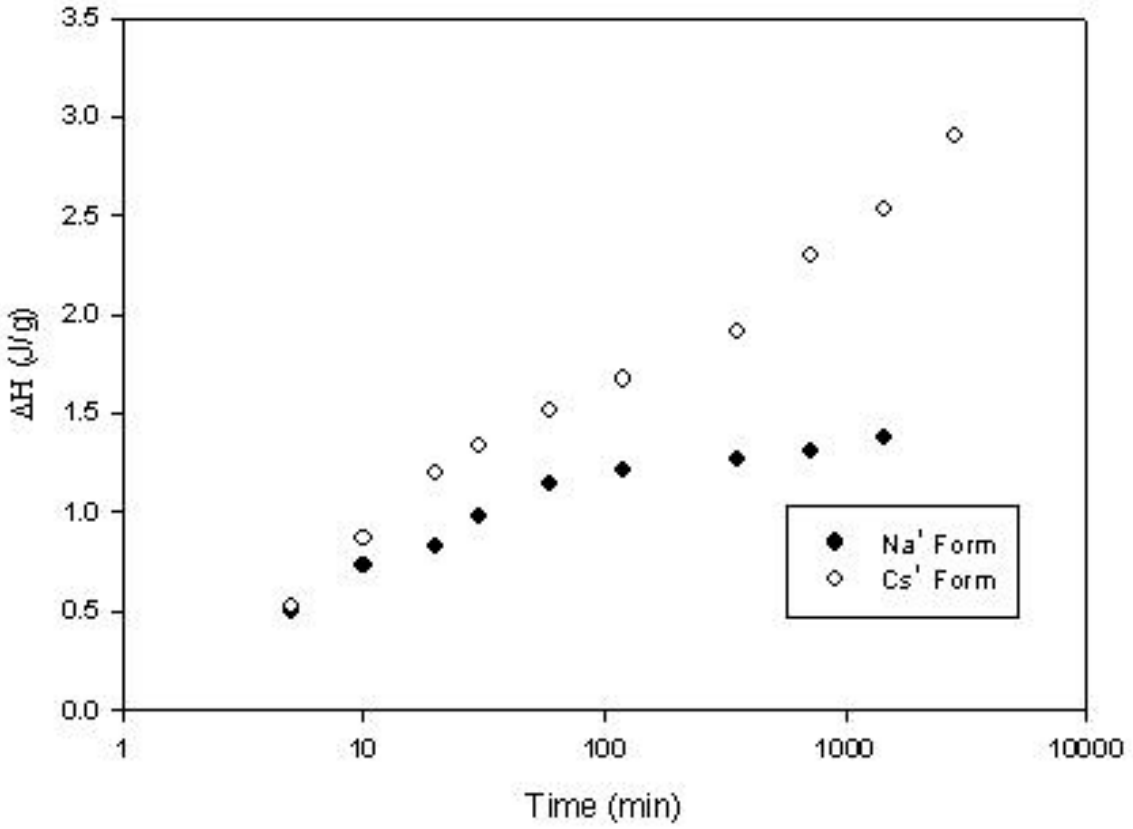

Figure 3.5 Heat of fusion (ΔH) values of Na^+- and Cs^+-form Nafion® membranes annealed at 200°C

As can be seen from Figure 3.5, for both Na^+-form and Cs^+-form Nafion® membranes, upon annealing at 200ºC, the value of ΔH start growing rapidly first with increasing annealing time and then the growing rate gradually slows down after annealing at 200ºC for one hour. Figure 2.3 also shows that when using Cs^+, which has a larger atomic size than Na^+ from the same group, as counterion, the samples develop higher ΔH values than that of their Na^+-form Nafion® counterparts after annealing at 200ºC. For the Na^+-form Nafion® samples, the ΔH value reaches a plateau of about 1.4J/g over extended period of time, while for the Cs^+-form Nafion® membranes,

the ΔH value after annealing at 200ºC for two days (2880 minutes) is 2.9J/g. This observation is in good agreement with the study on sulfonated syndiotactic polystyrene[13,14]. The larger ion Cs^+ results in weaker electrostatic crosslinks and therefore increases chain mobility, favoring the development of crystallinity.

B. DSC Results for Tetraalkylammonium-form Nafion® Samples

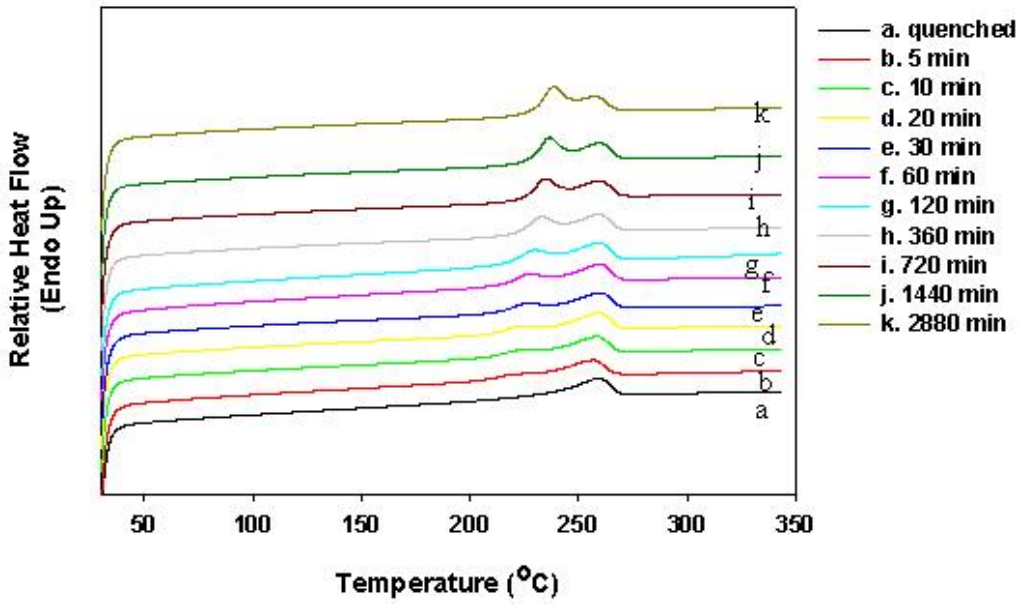

Figure 3.6 DSC thermograms of TMA^+-form Nafion® membranes, quenched rescan and annealed at 200°C for various periods of time. For comparison, the thermograms are shifted along the y axis.

Figure 3.6 shows the DSC results for TMA^+-form Nafion® membranes after thermal treatments. A peak is constantly present at around 259ºC. The position and shape of this peak, as well as the area under it, do not change with increasing annealing time. Park[15] attributed this peak to the packing of ordered counterions within the ionic clusters. In DSC analysis of TMA^+-, TEA^+-, TPA^+- and TBA^+- form Nafion® 117 without annealing, Park observed a systematic shift

of this endotherm to lower temperature from 260°C (TMA^+-form) to 180°C (TEA^+-form), 125°C (TPA^+-form) and 65°C (TBA^+-form) with increasing counterion size. WAXD and SAXS results of tretraalkylammonium-form Nafrion® 117 annealed directly from room temperature were used as additional support for this attribution. On the low angle side of the amorphous halo, the WAXD curves show a shoulder that shifts to lower angle with increasing counterion size. For TMA^+- and TEA^+-form Nafion®, the intensity and sharpness of this peak increase significantly with increasing annealing temperature. WAXD curve of TMA^+-form Nafion® annealed at high temperature also shows extra sharp peaks at 17.5° 2θ and 25° 2θ, similar to that observed with small molecular TMA^+ sulfonate salts. On the other hand, for TPA^+- and TBA^+-form Nafion®, the shoulder on the low angle side of the amorphous halo is insensitive to annealing temperature. SAXS results of TBA^+-form Nafion® show that annealing at 150°C causes a slight shift of the ionomer peak towards higher q, while annealing at 200°C does not further modify the curve significantly. SAXS results of TMA^+-form Nafion® annealed at 200°C, on the other hand, show a much narrower ionomer peak, suggesting a narrower distribution of the ionic domain separations. Alternatively, similar DSC behaviors have been observed in other copolymer systems, such as ethylene/1-octene copolymers[4], bisphenol-A polycarbonate[16] and ethylene/styrene copolymers[17], which have no counterion associated with them, and the two endothermic peaks are attributed to the melting of two distinct populations of crystals with the low endotherm associated with secondary crystals. Without further observations, we are unable to definitively distinguish between these two alternatives.

After annealing at 200°C a peak, more visible than that of the alkali metal-form Nafion® samples, appears above the annealing temperature and the magnitude of the peak increases with increasing annealing time, showing the development of ordering in the membrane during the

thermal annealing. Similarly, as noted in the results presented previously for the alkali metal-form Nafion® membranes, the position of the peak maximum shifts to higher temperature when annealed for longer periods of time. Figure 3.7 summarizes the change in the position of the endothermic peak.

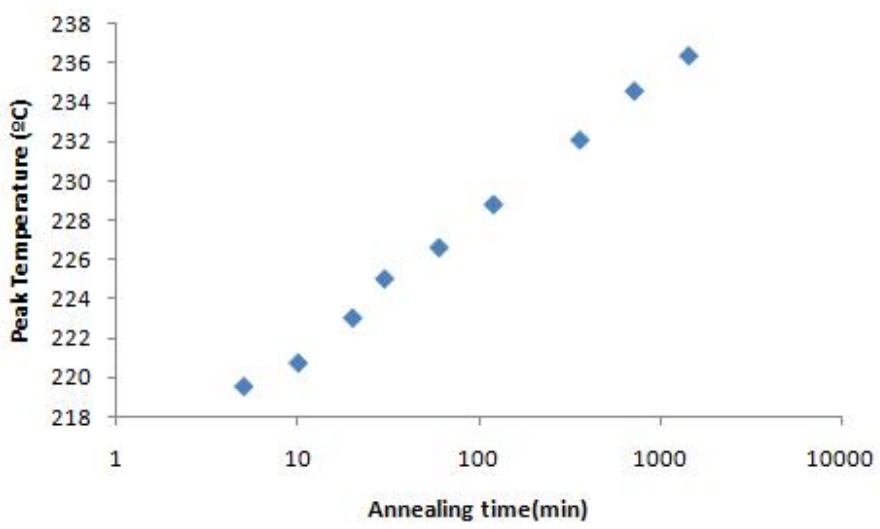

Figure 3.7 Change in peak temperature of TMA^+-form Nafion®

The heat of fusion, ΔH, of the low endothermic event is calculated by integration. The results are showed in Figure 3.8.

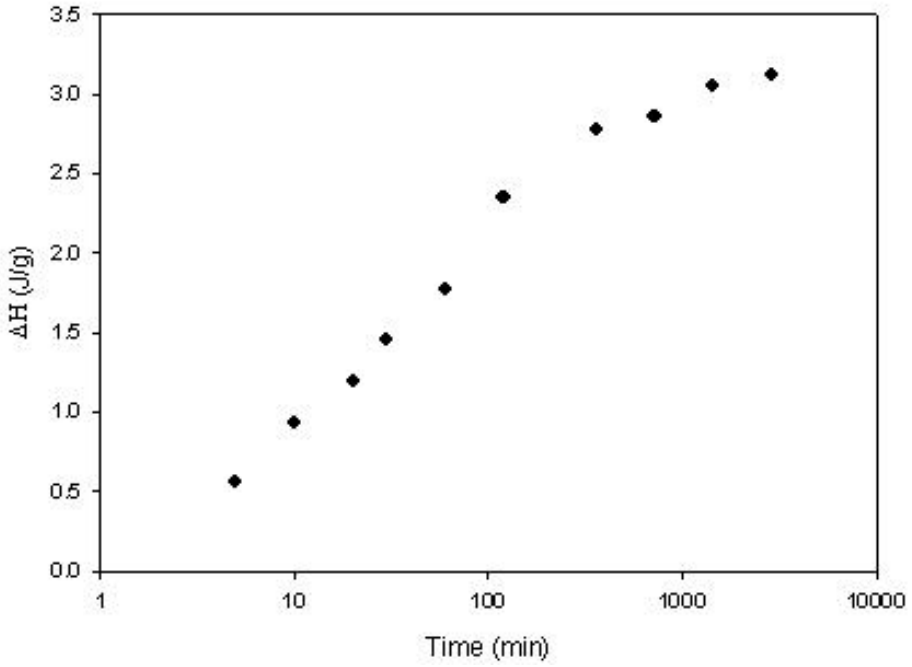

Figure 3.8 Heat of fusion (ΔH) values of TMA^+-form Nafion® membranes annealed at 200°C for various periods of time

As can be seen from Figure 3.8, for TMA^+-form Nafion® membranes, upon annealing at 200ºC, the value of ΔH also start growing rapidly first with increasing annealing time and then the growing rate gradually slows down after annealing at 200ºC for one hour. The TMA^+-form Nafion® membranes develop higher ΔH values than that of alkali metal-form Nafion® samples after annealing at 200ºC. For the TMA^+-form Nafion® samples, over extended annealing time the ΔH value reaches 3.05J/g, which is higher than the highest values reached for both the Na^+-form and Cs^+-form Nafion® membranes.

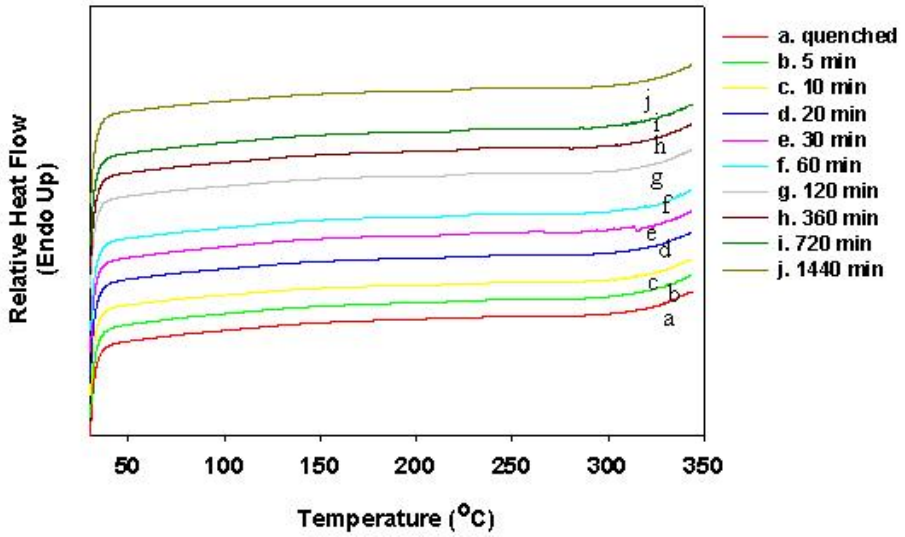

Figure 3.9 DSC thermograms of TEA^+-form Nafion® membranes, quenched rescan and annealed at 200°C for various periods of time. For comparison, the thermograms are shifted along the y axis.

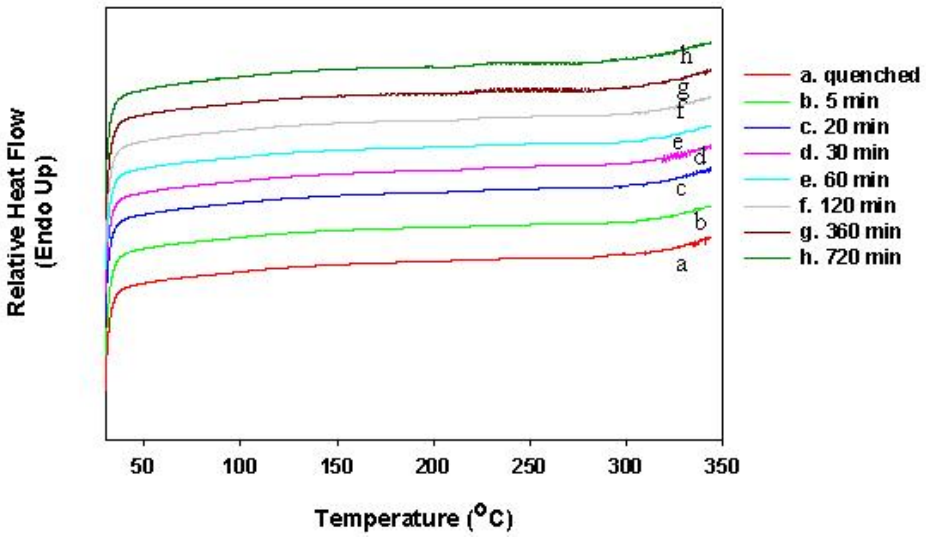

Figure 3.10 DSC thermograms of TPA^+-form Nafion® membranes, quenched rescan and annealed at 200°C for various periods of time. For comparison, the thermograms are shifted along the y axis.

Figure 3.9 and Figure 3.10 show the DSC results for TEA^+-form and TPA^+-form Nafion® membranes after thermal treatments. In the DSC thermogram of as-received TEA^+-form Nafion® membrane, there is a peak between 160ºC and 200ºC. This peak disappears upon heating at 330ºC and quenching back to room temperature. Unlike TMA^+-form Nafion® membranes, neither the TEA^+-form nor the TPA^+-form show any peak similar to the one at around 259°C observed in the DSC thermograms of TMA^+-form Nafion®. While for the TMA^+-form Nafion® membranes, an endothermic peak grows upon annealing at 200ºC and has higher ΔH than that of the alkali metal-form Nafion® samples, the DSC results for TEA^+-form and TPA^+-form Nafion® membranes show no observable peak upon annealing at 200°C, indicating that the growth in crystallinity during the annealing process is less significant for Nafion® membranes with larger tetraalkylammonium as counterions. Unlike the DSC thermograms of Na^+- , Cs^+- and TMA^+-form Nafion® membranes, the curves in these two figures show a rise in heat flow at temperature close to 350°C, indicating there are changes, possibly degradation, taking place at high temperatures in the less stable TEA^+-form and TPA^+-form Nafion® samples.

IV. Conclusions

Previous history and crytallinity in the as-received Nafion® membranes were eliminated by heating at 330ºC for 3 minutes, samples were then subject to annealing at 200°C for various periods of time. For both Na^+- and Cs^+-form Nafion® membrane, upon annealing at 200ºC, an endothermic peak appears above the annealing temperature. The position of the peak maximum shifts to higher temperature when annealing time is increased. The ΔH value of the endothermic

event increases rapidly with increasing annealing time before slowing down gradually when annealed for extended times higher than 60 minutes, showing the development of crystallites in the membranes during the annealing process. The annealed Cs^+-form Nafion® samples have higher ΔH values than their Na^+-form counterparts. The ΔH value of the Na^+-form Nafion® reaches a plateau of approximately 1.37J/g, and that of the Cs^+-form Nafion® reaches 2.90J/g upon annealing at 200ºC for 2 days. This suggests that the counterion associated with the sulfonate groups can affect the development of crystallinity, possibly because the counterion has an effect on the cross-links formed by the sulfonate groups.

For TMA^+-form Nafion® membranes, the DSC results show a peak at around 259ºC that is not affected by annealing time. Upon annealing at 200ºC, a low endothermic peak appears and the position of the peak maximum shifts to higher temperature with increasing annealing time. The ΔH value of this endothermic event increases rapidly with annealing time at first and then gradually reaches a maximum of 3.06J/g, which is higher than that of the alkali metal-form Nafion® membranes. Park[15] attributed the high endothermic peak to the packing of ordered counterions within the ionic clusters. On the other hand, similar DSC behaviors have been observed in other copolymer systems and the two peaks are attributed to two distinct populations of crystals[4,16,17].

The DSC results for TEA^+- and TPA^+-form Nafion® membranes, however, show no peak similar to the one at around 259ºC observed in the DSC results of TMA^+-form Nafion® membranes and no observable peak emerging upon annealing at 200ºC for various periods of time, indicating that there is ether no significant development of crystallinity during the isothermal process. This again suggests that the counterion can have a significant effect of the crystallization process in the membrane. While the trend in the heat of fusion of Na^+-, Cs^+- and

TMA^+-form Nafion® can be explained in term of counterion size, as larger counterion destabilize the electrostatic cross-link, the DSC results of annealed TEA^+- and TPA^+-form Nafion® samples do not follow the same pattern. One speculation is that these larger organic counterions that are tightly bound to the side chains yield extremely bulky defects, which disrupt the ability of TFE units between these defects to organize into tightly packed crystallites. However, further studies are needed in order to fully explain this behavior.

Reference

1. Marand, H.; Alizadeh, A.; Farmer, R.; Desai, R.; Velikov, V. *Macromolecules* **2000**, *33*, 3392-3403.
2. Alizadeh, A.; Sohn, S.; Quinn, J.; Marand, H.; Shank, L. C.; Iler, H. D. *Macromolecules* **2001**, *34*, 4066-4078.
3. Flory, P. J. *Trans. Faraday Soc.* **1955**, *51*, 848-857.
4. Alizadeh, A.; Richardson, L.; Xu, J. ; McCartney, S.; Marand, H.; Cheung, Y. W.; Chum, S. *Macromolecules* **1999**, *32*, 6221-6235.
5. Alamo, R. G.; Mandelkern, L. *Thermochimica Acta* **1994**, *238*, 155-201.
6. Sanchez, I. C.; Eby, R. K. *Macromolecules* **1975**, *8*, 638-641.
7. Gierke, T. D.; Munn, G. E.; Wilson, F. C. *J. Polym. Sci. Pt. B-Polym. Phys.* **1981**,*19*, 1689-1704
8. Fujimura, M.; Hashimoto, T.; Kawai, H. *Macromolecules* **1981**, *14*, 1309-1315.
9. Gebel, G.; Aldebert, P.; Pineri, M. *Macromolecules* **1987**, *20*, 1425-1428.
10. Roche, E. J.; Pineri, M.; Duplessix, R.; Levelut, A. M. *J. Polym. Sci. Pt. B-Polym. Phys.* **1981**, *19*, 1-11.

11. Lee, E. M.; Thomas, R. K.; Burgess, A. N.; Barnes, D. J.; Soper, A. K.; Rennie, A. R. *Macromolecules* **1992**, *25*, 3106-3109.

12. Page, K. A.; Cable, K. M.; Moore, R. B. *Macromolecules* **2005**, *38*, 6472-6484.

13. Orler, E. B.; Moore, R. B. *Macromolecules* **1994**, *27*, 4774-4779.

14. Orler, E. B.; Calhoun, B. H.; Moore, R. B. *Macromolecules* **1996**, *29*, 5965-5971.

15. Park, J. K. Ph.D. Dissertation **2009**, Virginia Tech.

16. Sohn, S.; Alizadeh, A.; Marand, H. *Polymer* **2000,** *41*, 8879-8886.

17. Huang, Z. Y.; Marand, H.; Cheung, W. Y.; Guest, M. *Macromolecules* **2004,** *37*, 9922-9932.

4. Isothermal Crystallization Kinetics of Nafion® Membranes in Different Counterion Forms

I. Introduction

The Avrami equation, proposed by Avrami[1-3] between 1939 and 1941, is a convenient way to describe the transformation of material from one phase to another at constant temperature. In particular, it can be used to describe isothermal crystallization kinetics of any type, as it requires no information regarding the molecular mechanism of the crystallization process.

It is assumed that crystallization starts randomly at various locations throughout the entire untransformed portion of the sample and the growth of crystallites is linear in space with a rate that is constant and not affected by the extent of transformation. With is simplification, the time evolution of the transformation of material can be described using the general Avrami equation:

$$1 - Y = \exp(-kt^n) \qquad 3\text{-}1$$

in which Y is the extent of transformation, k and n are constants. k is the temperature dependent bulk crystallization rate coefficient and is related to nucleation rate and growth rate, and an increase in n indicates higher "dimensionality" of the growth. A plot of lnln(1/1-Y) vs. ln(time) can be used to determine the values of n and k. According to the general Avrami equation, the slope of this plot is n and the y-intercept is lnk.

For low degree of crystallinity, the Avrami equation can be written as:

$$\Delta H = Kt^n \qquad 3\text{-}2$$

Equation 3-2 is used in order to describe the isothermal crystallization process of Na^+ -form and TMA^+-form Nafion® 117 samples.

II. Results

A. Na^+-form Nafion®

The plot of lnΔH vs. ln(time) is shown in Figure 4.1.

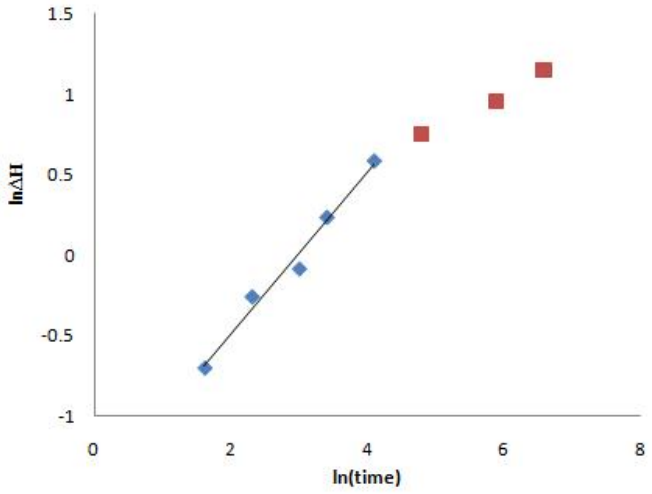

Figure 4.1 Evolution of endotherm for Na^+-form Nafion® at 200°C for different times

Using the linear relationship shown in Figure 4.1, and according to the Avrami equation at low crystallinity, the Avrami exponent is conclude to be about 0.5.

B. TMA^+-form Nafion®

The plot of lnΔH vs. ln(time) is shown in Figure 4.2.

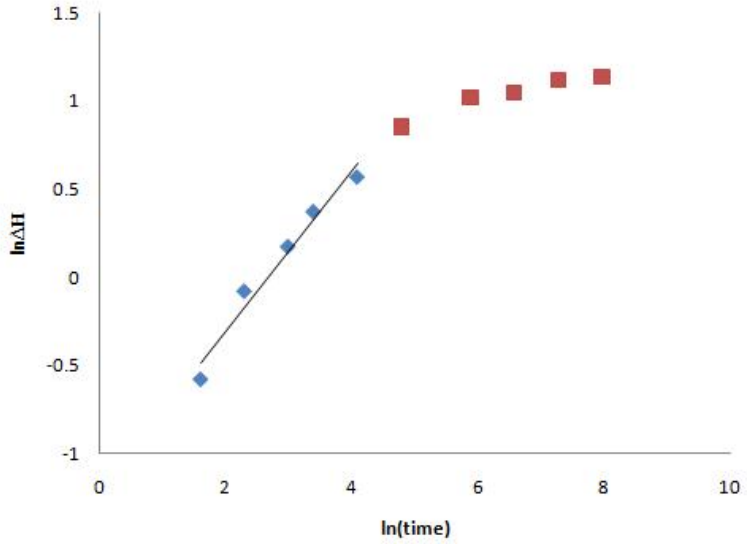

Figure 4.2 Evolution of endotherm for TMA^+-form Nafion® at 200°C for different times

Using the linear relationship shown in Figure 4.2, and according to the Avrami equation at low crystallinity, the Avrami exponent is conclude to be about 0.5.

IV. Conclusions

Avrami analysis was performed using isothermal crystallization data of Na^+-form and TMA^+-form Nafion® 117 samples. For the isothermal crystallization of both forms at 200ºC, the Avrami exponent n derived from Avrami analysis is about 0.5. This value of Avrami exponent has also been obtained from other polymer systems such as ethylene/1-octene copolymers[4] and Poly(arylene ether ether ketone)[5], and is characteristic of the early stage of secondary crystallization. Later stage of crystallization shows a deviation from n=0.5. While secondary crystallization in these systems is constrained between lamellae, the crystallization in ionomers such as PFSI might be similarly constrained between ionic domains.

References

1. Avrami, M. *J. Chem. Phys.* **1939**, *7*, *1103–1112*.
2. Avrami, M. *J. Chem. Phys.* **1940**, *8*, *212–224*.
3. Avrami, M. *J. Chem. Phys.* **1941**, *9*, *177–184*.
4. Alizadeh, A.; Richardson, L.; Xu, J. ; McCartney, S.; Marand, H.; Cheung, Y. W.; Chum, S. *Macromolecules* **1999**, *32*, 6221-6235.
5. Marand, H.; Alizadeh, A.; Farmer, R.; Desai, R.; Velikov, V. *Macromolecules* **2000**, *33*, 3392-3403.

5. Thermal Treatments on Perfluorosulfonate Ionomers with Shorter Side Chains and Various Equivalent Weights

I. Introduction

Dow Ionomer was a kind of perfluorosulfonate ionomer with a side chain shorter than that of Nafion® developed by Dow Chemical Company in the 1980s[1]. Tant et al.[2] reported that Dow Ionomer had a higher degree of crystallinity than at of Nafion® with comparable equivalent weight. Moore et al.[3] showed that similar to Nafion®, Dow polymer displays higher extent of crystallinity at higher equivalent weight.

3M has recently introduced an ionomer[4, 5] that has an intermediate side chain length between Nafion® and the Dow polymer. The equivalent weight of the 3M Ionomer is EW = 100 (n) + 377.

This section mainly focuses on the effects of thermal annealing on 3M Ionomer with different equivalent weights. Dow Ionomer is used at times for comparison purposes.

II. Experimental

DSC analysis was carried out on a TA Instruments Q2000 differential scanning calorimeter. Thermally annealed samples were scanned at a rate of 20°C/min to 350°C.

III. Results

A. Na^+-form 3M Ionomers

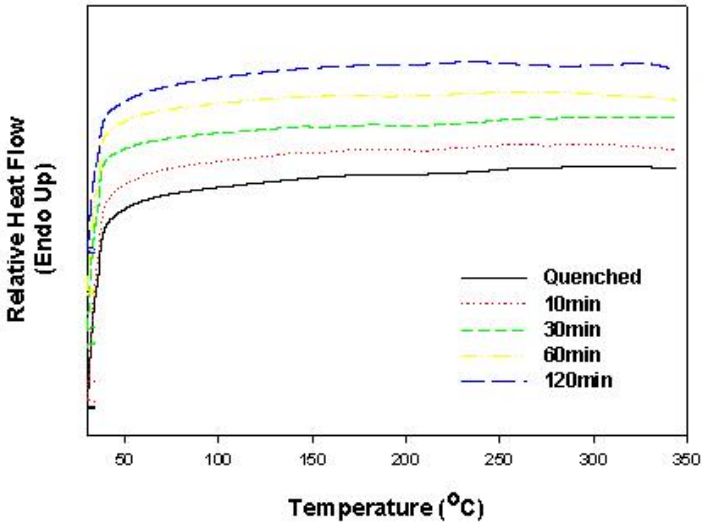

Figure 5.1 DSC thermograms of 700EW Na^+-form 3M Ionomer, quenched rescan and annealed at 200°C for various periods of time. For comparison, the thermograms are shifted along the y axis.

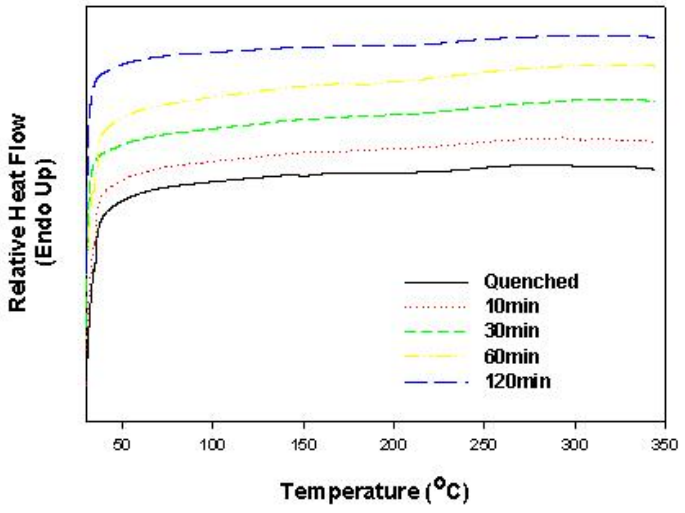

Figure 5.2 DSC thermograms of 800EW Na^+-form 3M Ionomer, quenched rescan and annealed at 200°C for various periods of time. For comparison, the thermograms are shifted along the y axis.

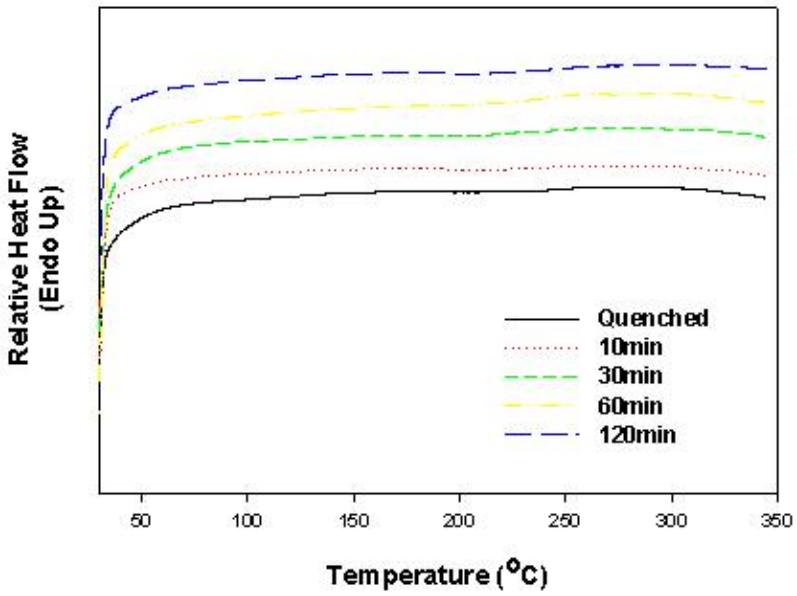

Figure 5.3 DSC thermograms of 900EW Na^+-form 3M Ionomer, quenched rescan and annealed at 200°C for various periods of time. For comparison, the thermograms are shifted along the y axis.

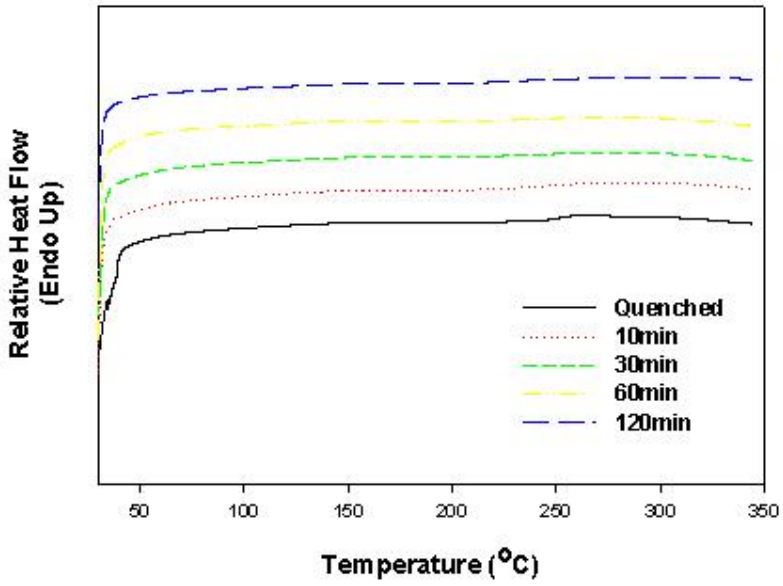

Figure 5.4 DSC thermograms of 1000EW Na^+-form 3M Ionomer, quenched rescan and annealed at 200°C for various periods of time. For comparison, the thermograms are shifted along the y axis.

Figure 5.1 – Figure 5.4 show the DSC results for Na^+-form 3M Ionomers with various equivalent weights after annealing at 200ºC for various periods of time. Even though higher equivalent weight often favors crystallization, in all four graphs, including the one for Na^+-form 3M Ionomer samples with 1000EW (13.8 mole% of side chains), no peak can be observed, indicating that for these samples, little amount of ordering can develop upon annealing at 200ºC, which is very different from the DSC results of annealed Na^+-form Nafion® 117, which has a slightly lower mole fraction of side chains, 13.2%. For Na^+-form Nafion® 117 samples, when annealed at 200ºC, an endothermic peak appears and the value of ΔH increases rapidly with increasing annealing time when annealing time is small, and the gradually reaches a plateau after annealing for more than one hour.

B. TMA^+-form 3M Ionomers

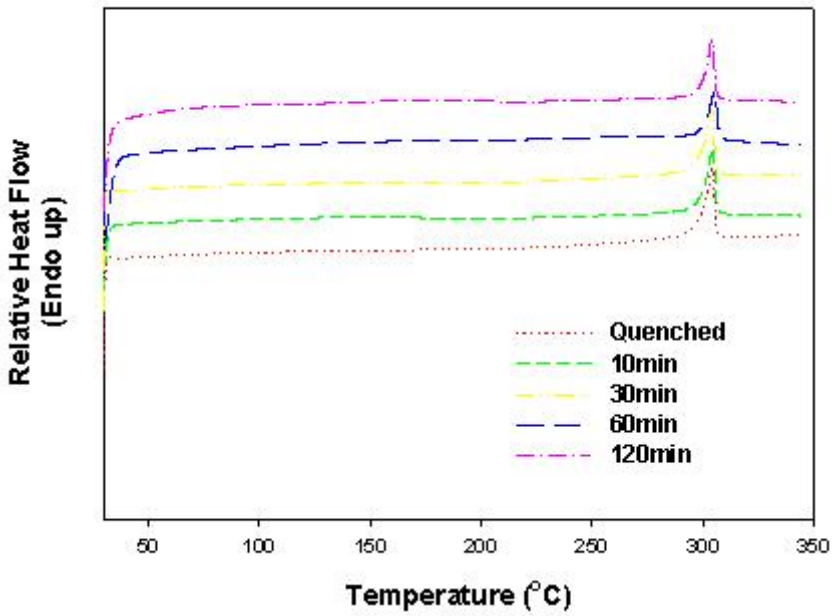

Figure 5.5 DSC thermograms of 700EW TMA^+-form 3M Ionomer, quenched rescan and annealed at 200°C for various periods of time. For comparison, the thermograms are shifted along the y axis.

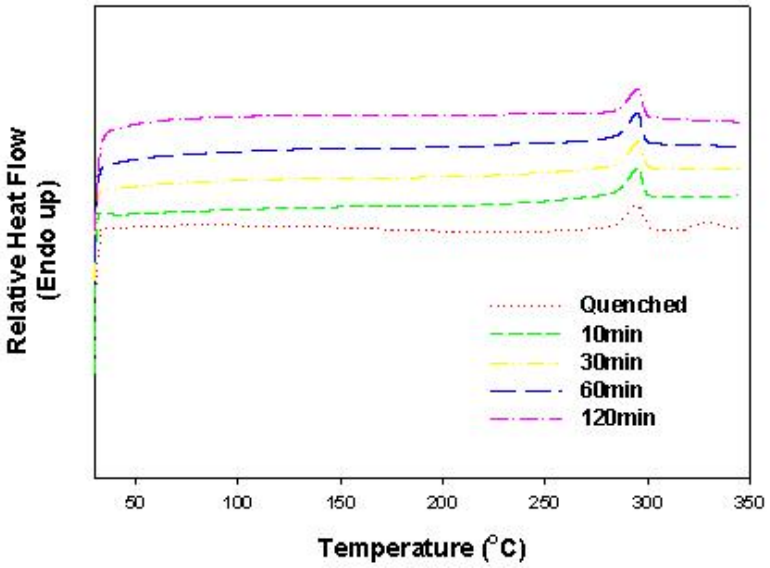

Figure 5.6 DSC thermograms of 800EW TMA^+-form 3M Ionomer, quenched rescan and annealed at 200°C for various periods of time. For comparison, the thermograms are shifted along the y axis.

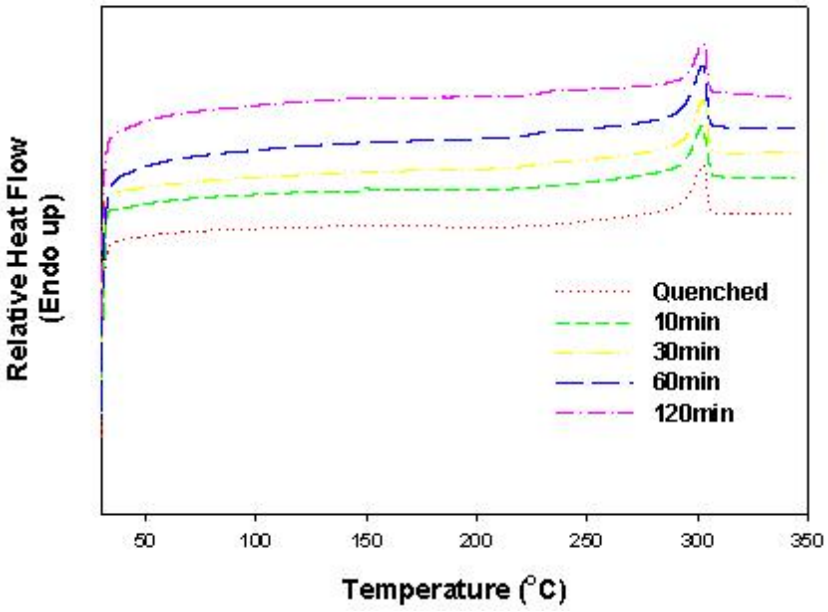

Figure 5.7 DSC thermograms of 900EW TMA^+-form 3M Ionomer, quenched rescan and annealed at 200°C for various periods of time. For comparison, the thermograms are shifted along the y axis.

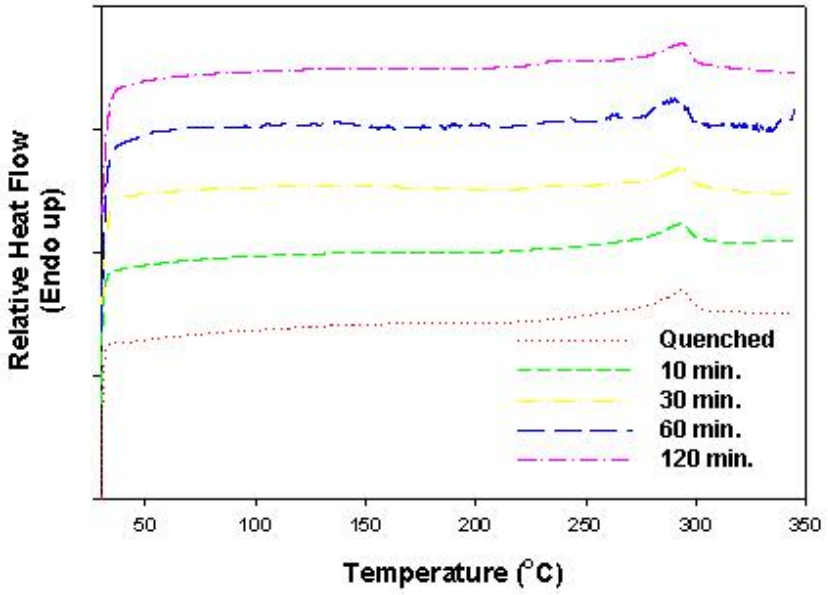

Figure 5.8 DSC thermograms of 1000EW TMA^+-form 3M Ionomer, quenched rescan and annealed at 200°C for various periods of time. For comparison, the thermograms are shifted along the y axis.

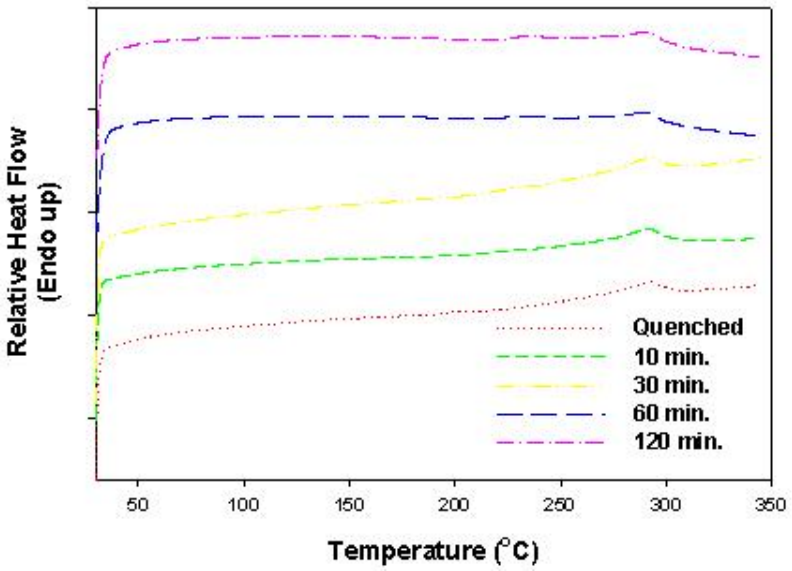

Figure 5.9 DSC thermograms of 1100EW TMA^+-form 3M Ionomer, quenched rescan and annealed at 200°C for various periods of time. For comparison, the thermograms are shifted along the y axis.

Figure 5.5 – Figure 5.9 show the DSC thermograms of 700, 800, 900, 1000 and 1100EW TMA^+-form 3M Ionomers annealed at 200°C for various periods of time. While there is a peak constantly present in all thermograms of TMA^+-form Nafion® 117 membranes at around 259ºC, in TMA^+-form 3M ionomers, for TMA^+-form 3M ionomers this peak maximum is located at higher temperature between 292ºC and 304ºC, depending on the equivalent weight of the sample, and the shape of the peak is sharper for smaller equivalent weight. The location of the peak maximum shifts slightly to lower temperatures with increasing equivalent weigh, except for the 800EW sample, which has a constant endothermic peak at temperature lower than that of the endothermic peak for the 900EW sample. It should be noted that according to 3M, the 800EW 3M ionomer sampler was cast out of a different solvent (methanol) than other samples, which were cast out of n-propanol. The 800EW 3M Ionomer sample was also dried under slightly different conditions by 3M. Therefore, the position of this endothermic peak might be affected

by the casting and drying conditions of the sample. However, further conclusions cannot be drawn without knowing more detailed information regarding how 3M processed the samples.

For 700EW TMA^+-form 3M Ionomer, which has a 23.6 mole% of side chains, in the DSC thermograms presented in Figure 5.5, no peak can be seen grow in upon annealing at 200ºC. As the mole% of branch decreases, a new peak appears after annealing at 200ºC, and the ΔH value increases with increasing annealing time or decreasing mole% of branch, which is expected, for lower mole% of branch means larger fraction of the PTFE-like backbone. However, the growth of the ΔH value with increasing annealing time is small comparing to that of TMA^+-form Nafion® 117, and after annealing at 200ºC for 2 hours, the ΔH value of the 1100EW (12.2 mole% of branch) TMA^+-form 3M Ionomer is only about 0.62J/g, which is significantly smaller than that of its Nafion® 117 counterpart, which has a larger mole% of side chains of 13.2.

C. 1100EW TEA^+-form 3M Ionomer

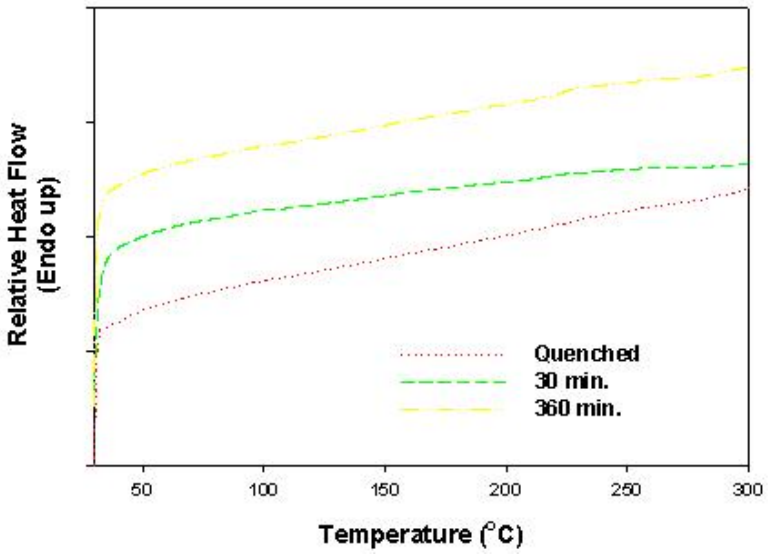

Figure 5.10 DSC thermograms of 1100EW TEA^+-form 3M ionomer, quenched rescan and annealed at 200°C for various periods of time. For comparison, the thermograms are shifted along the y axis.

Similar to TEA^+-form Nafion® 117, DSC thermograms of the annealed 1100EW (12.2 mole% of side chains) TEA^+-form 3M Ionomer only show an observable peak after annealing for extended period of time, and the ΔH value of the endothermic event is very small. This suggests that there is extremely low degree of ordering developed in the membrane during the annealing process at 200°C.

D. TMA^+-form Dow Ionomers

Figure 5.11 – Figure 5.13 show the DSC thermograms of TMA^+-form 606, 793, 1040EW Dow Ionomers annealed at 200ºC for various times. While there is a peak constantly present in all thermograms of TMA^+-form Nafion® 117 membranes at around 259ºC, and of TMA^+-form 3M Ionomers with various EW at 292-304ºC, the peak maximum of TMA^+-form Dow polymers is located at lower temperatures between 240ºC and 261ºC. Similar to 3M Ionomer, the peak also become broader with increasing equivalent weight and the peak maximum shifts to lower temperature as equivalent weight increases, although the shift is much more significant than that of the 3M Ionomer samples.

Upon annealing at 200ºC a new peak grows in, the ΔH value increases with increasing equivalent weight, with the ΔH value of the 1040EW (11.6 mole% of side chains) sample after annealed at 200ºC for 6 hours higher than that of TMA^+-form Nafion® 117(13.2 mole% of side chains). This result is reasonable considering that the lower mole% of branch means higher fraction of crystallizable tetrafluoroethylene units. It also has to be noted that Moore and Martin[3] proposed that based on their observation that the melting point of Dow Ionomers varied only slightly throughout a range of different equivalent weights, the Dow Ionomers are more of a series of block-type copolymers. This nature of the Dow Ionomers may also contribute to the higher degree of crystallinity developed upon annealing at 200°C of these samples.

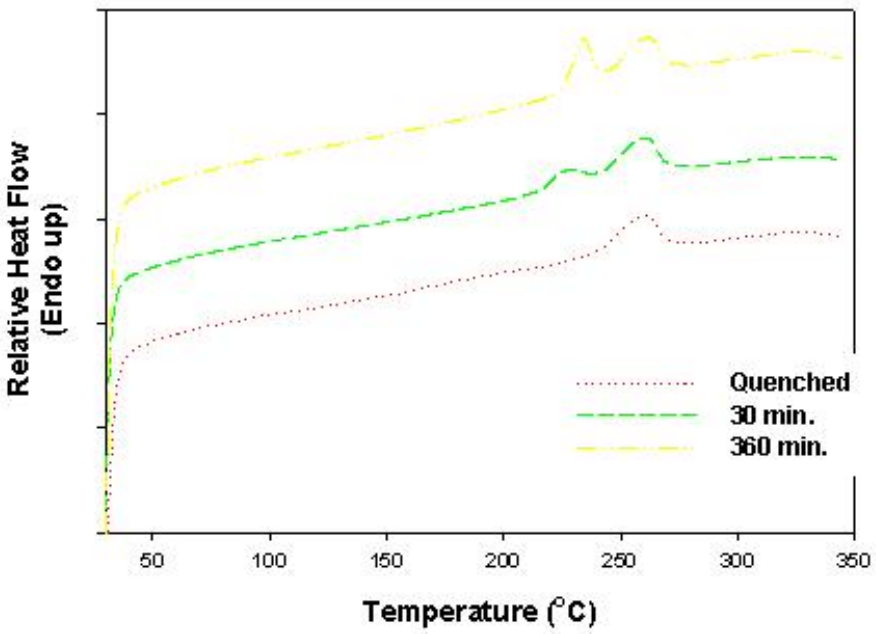

Figure 5.11 DSC thermograms of 606EW TMA^+-form Dow Ionomer, quenched rescan and annealed at 200°C for various periods of time. For comparison, the thermograms are shifted along the y axis.

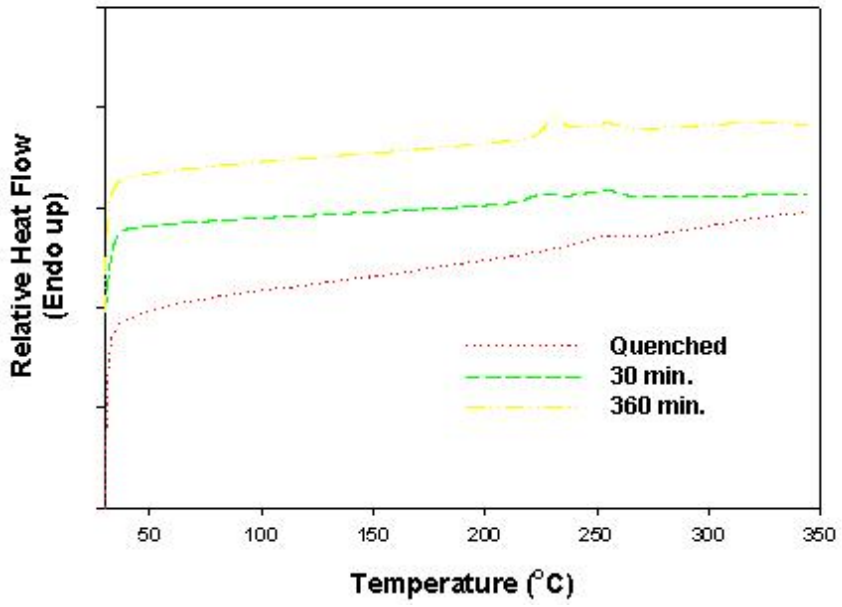

Figure 5.12 DSC thermograms of 793EW TMA^+-form Dow Ionomer, quenched rescan and annealed at 200°C for various periods of time. For comparison, the thermograms are shifted along the y axis.

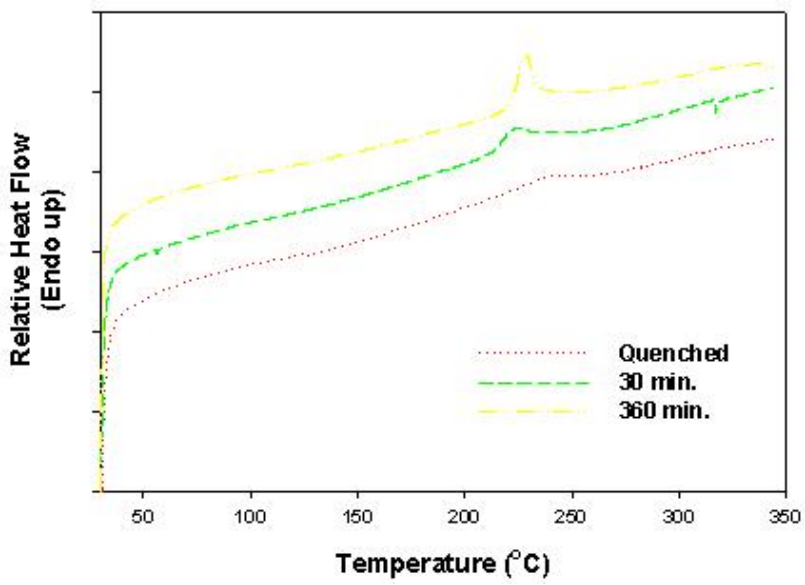

Figure 5.13 DSC thermograms of 1040EW TMA^+-form Dow Ionomer, quenched rescan and annealed at 200°C for various periods of time. For comparison, the thermograms are shifted along the y axis.

IV. Conclusions

An endothermic peak is constantly present in the DSC thermograms of all TMA^+-form membranes. The peak is located at around 259ºC for TMA^+-form Nafion® 117, at lower temperatures for TMA^+-form Dow Ionomers, which have shorter side chains, and at higher temperatures for TMA^+-form 3M Ionomers, which have intermediate side chains. Within the same type of samples, the position of the peak maximum shifts to lower temperature and the peak becomes broader with increasing equivalent weight. It seems that the position and shape of this peak is related to equivalent weight and length of side chains. Park[6] attributed this high endothermic peak to the packing of ordered counterions within the ionic cluster, while similar DSC behaviors have been observed in other copolymer systems and the two endotherms are attributed to two distinct populations of crystals[7-9].

While some consider shorter side chains favorable for the development of crystallinity in PFSI membranes, this matter appears to be complicated according to the results presented in this chapter. Thermograms of Na^+-form 3M Ionomers show no peak upon annealing at 200ºC, while Na^+-form Nafion® 117 membranes develop an endothermic peak that can be attributed to the development of crystallinity. The ΔH value of 1100EW TMA^+-form 3M Ionomer (12.2 mole% of side chains) after annealed at 200ºC for two hours is significantly smaller than that of its TMA^+-form Nafion® 117 counterpart (13.2 mole% of side chains). On the other hand, the ΔH value 1040EW TMA^+-form Dow Ionomer after annealing at 200ºC for 6 hours are higher than that of TMA^+-form Nafion® 117. The 1040EW Dow Ionomer has 11.6 mole% of side chains, which is lower than that of Nafion® 117, meaning that the Dow Ionomer has a higher fraction of crystallizable tetrafluoroethylene units. In the case of the Dow Ionomers, it has to be noted that based on DSC study done by Moore and Martin[3], they are more of block copolymers than real random copolymers.

References

1. Ezzell, B. R.; Carl, W. P.; Mod, W. A., Novel polymer having acid functionality. Patent US4330654, **1982**.
2. Tant, M. R.; Lee, K. D.; Darst, K. P.; Martin, C. W. *Polymer Materials: Science and Engineering* **1988**, *58*, 1074-1078.
3. Moore, R. B.; Martin, C. B. *Macromolecules* **1989**, *22*, 3594-3599.
4. Guerra, M. A. Preparation of perfluorinated vinyl ethers having a sulfonyl fluoride end-group. Patent US6624328, **2003**.

5. Hamrock, S. J.; Rivard, L. M.; Innes Moore, G. G.; Freemyer, H. T., Polymer electrolyte membrane. Patent Application US29949121219, **2004**.
6. Park, J. K. Ph.D. Dissertation **2009**, Virginia Tech.
7. Alizadeh, A.; Richardson, L.; Xu, J. ; McCartney, S.; Marand, H.; Cheung, Y. W.; Chum, S. *Macromolecules* **1999**, *32*, 6221-6235.
8. Sohn, S.; Alizadeh, A.; Marand, H. *Polymer* **2000**, *41*, 8879-8886.
9. Huang, Z. Y.; Marand, H.; Cheung, W. Y.; Guest, M. *Macromolecules* **2004**, *37*, 9922-9932.

6. Water Uptake of Annealed TMA^+-form Nafion® Membranes

I. Introduction

Water content, λ, is defined as the number of moles of water per every mole of sulfonate group. Therefore, the water content λ of a Nafion® Membrane can be calculated using Equation 5-1:

$$\lambda = \frac{\frac{mass\ of\ water\ in\ the\ membrane}{18 g/mole}}{\frac{mass\ of\ the\ dry\ membrane}{EW}} \qquad 5\text{-}1$$

in which EW is the equivalent weight of the membrane. The ability of a PFSI membrane to absorb water is known to have an effect on the performance of the membrane in a fuel cell and it has been reported that higher water content in a membrane results in an increase in the conductivity of the membrane[1, 2].

The objectives of this chapter are to investigate the water uptake of TMA^+-form Nafion® 117 membranes annealed at 200ºC for various periods of time and the possible correlation between water uptake and the degree of crystallinity.

II. Experimental

A. Materials

Nafion® 117 CS membranes (1100 g/mol SO_3^- equivalent weight, sulfonic acid form) were obtained from E. I. du Pont de Nemours and Company. Tetramethylammonium hydroxide (TMAOH), 1.0M aqueous solution was obtained from Alfa Aesar and used without further purification.

B. Preparation of Nafion® 117 Membranes

The Nafion® membranes were boiled in 8M nitric acid (HNO_3) solution under reflux for two hours in order to remove impurities. The membranes were then rinsed in deionized water three times and boiled in deionized water for another hour. After cleaning the membranes were dried in vacuum oven at 70°C overnight.

C. Counterion Exchange

The cleaned H^+-form membranes were stirred in excess tetramethylammonium hydroxide (TMAOH) solution for 24 hours. The membranes were then rinsed in methanol three times and stirred in methanol for 12 hours before they were dried in vacuum oven at 70°C overnight.

D. Thermal Treatments

The TMA^+-form Nafion® 117 membranes were heated at 330°C for three minutes to erase previous history of the samples. The membranes were then annealed at 200°C for various periods of time ranging from 5 minutes to 12 hours.

E. Water Uptake Experiment

The dry weights of the membranes were measured after drying the samples at 70°C overnight in vacuum oven. The membranes were then boiled in deionized water for 1 hour. After boiling the membranes were dipped into deionized water before their wet weights were measured. The mass of water in a membrane was calculated by subtracting the dry weight of the membrane from the wet weight of the membrane, and water content values were calculated using Equation 5-1. Multiple samples were measured in order to make sure the results are reproducible and the experimental errors are within reasonable range.

III. Results and Discussions

Annealing time(min)	Water content, λ	Standard deviation
0	19.9	1.99
5	21.3	3.14
10	19.3	1.66
20	16.9	1.56
30	15.4	0.68
60	16.1	0.92
120	15.1	1.13
360	16.1	0.71
720	15.4	1.53

Table 6-1 Water content values of TMA^+-form Nafion® 117 membranes annealed at 200°C for various periods of time

Table 5-1 shows the results of water uptake analysis of TMA^+-form Nafion® 117 membranes annealed at 200ºC for various periods of time. To better illustrate the results, water content values was plotted vs. annealing time on the graph of the ΔH vs. annealing time, plotted using data from Chapter 2.

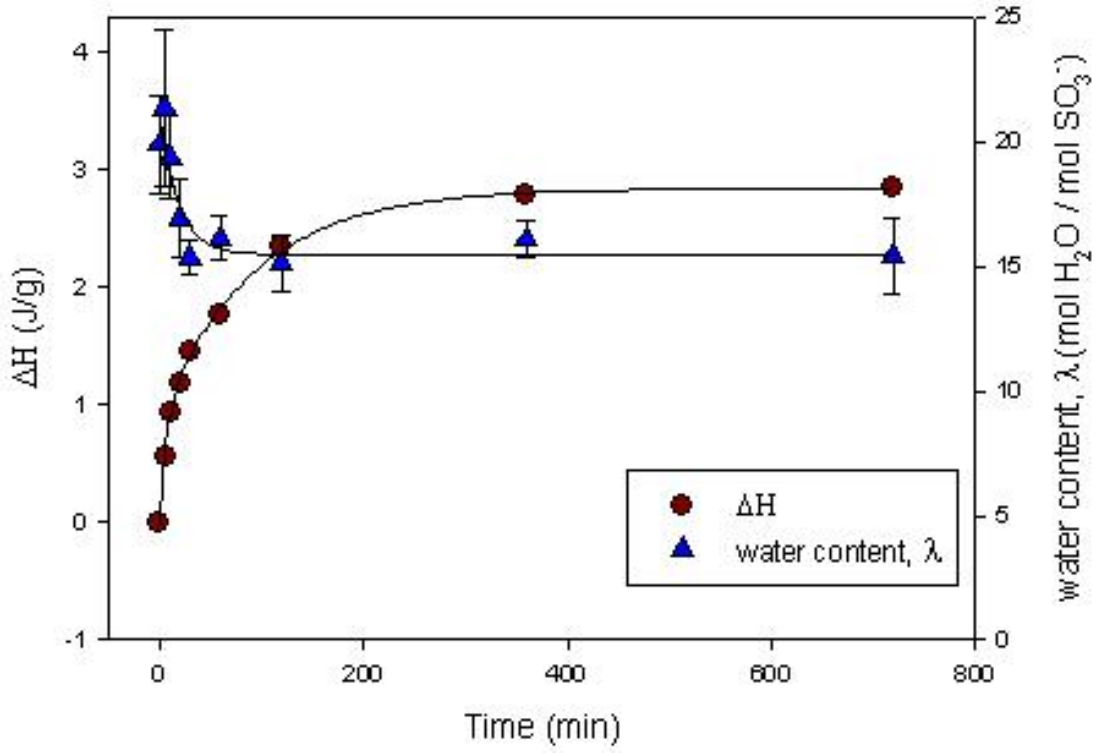

Figure 6.1 Water uptake measurement and heat of fusion (ΔH) values of TMA^+-form Nafion® membranes annealed at 200°C for various periods of time

As can be seen from Figure 5.1, at the beginning the water content decreases rapidly with increasing annealing time, and then reaches a low plateau after annealing at 200ºC for 2 hours or longer. It is noteworthy that the change in the water uptake with increasing annealing time mirrors the change in ΔH value, with ΔH increases rapidly with annealing time and then reaches a high plateau after annealing at 200ºC for 2 hours or longer. These results suggest that although the degree of crystallinity is small in these thermally annealed Nafion® membranes, it may have a significant effect on important properties of the membranes. It has been proposed that the

crystalline domains in Nafion® may act as barriers to solvent swelling[3], and the change in the water uptake of the annealed membranes shown in Figure 5-1 is in agreement with this thought.

References

1. Zawodzinski, T. A.; Derouin, C.; Radzinski, S. et al. *Journal of The Electrochemical Society* **1993**, *140*, 1041-1047.
2. Zawodzinski, T. A.; Davey, J.; Valerio, J.; Gottesfeld, S. *Electrochimica Acta* **1995**, *40*, 297-302.
3. Mauritz, K. A.; Moore, R. B. *Chem. Rev.* **2004**, *104*, 4535-4585.

7. Conclusions and Future Work

I. Conclusions

The effects of thermal annealing on different counterion-forms of Nafion® 117 as well as 3M ionomers and Dow polymers with various equivalent weights are studied. After heating at 330ºC for 3 minumtes, upon annealing at 200ºC for various amount of time, DSC thermograms of Na^+-, Cs^+- and TMA^+-form Nafion® 117 membranes show an endothermic peak growing in and the ΔH value of the endothermic event increases with increasing annealing time until it reaches a plateau over extended periods of time, indicating the development of crystallinity in the membrane. Among these three forms, the TMA^+-form has the highest value of ΔH and Na^+-form the lowest. On the other hand, other tetraalkylammonium forms of Nafion® 117 do not develop any endothermic peak upon annealing at 200ºC for various times, suggesting there is either no or little crystallinity developed during the annealing process at 200ºC. These results confirm that the types of counterion can significantly affect the isothermal crystallization process of Nafion®.

DSC thermograms of Na^+-form 3M ionomers show no peak upon annealing at 200ºC, while DSC results of TMA^+-form 3M ionomers at high equivalent weights (low mole% of side chains) show an endothermic peak develop upon annealing at 200ºC. The ΔH value, though, is significantly smaller than that of TMA^+-form Nafion® 117 annealed under same conditions. On the other hand, 1040EW TMA^+-form Dow polymer (11.6 mole% of side chains), which is more of a block polymer than a true random copolymer, after annealing at 200ºC for 6 hours are higher than that of TMA^+-form Nafion® 117 (13.2 mole% of side chains). Apart from the blocky nature, the lower mole% of branch can also contribute to the higher degree of crystallinity developed during isothermal crystallization. These results indicate that the effect of chain length on the

isothermal crystallization kinetics of the membrane might be a complicated matter. Both the chain length and the counterion associated with the sulfonate groups may contribute, and the nature of the ionomer also has to be taken into account. To obtain further information regarding this matter, ideally, different types of PFSI with same or comparable mole% of branch should be used for comparision.

An endothermic peak is constantly present in the DSC thermograms of all TMA^+-form membranes. The peak is located at around 259ºC for TMA^+-form Nafion® 117, at temperatures between 240ºC and 261ºC for TMA^+-form Dow polymers, which have shorter side chains, and at temperatures between 292ºC and 304ºC for TMA^+-form 3M ionomers, which have intermediate side chains. Within the same type of samples, the position of the peak maximum shifts to lower temperature and the peak becomes broader with increasing equivalent weight. It seems that the position and shape of this peak is related to equivalent weight and length of side chains. Park[1] attributed this high endotherm in Nafion® to the packing of counterions within the ionic cluster, while similar DSC patterns have be observed in various polymer systems and the two endotherms are attributed to two distinct population of crystals with the low endotherm associated with secondary crystals[2-4].

Water uptake analysis was performed on TMA^+-form Nafion® 117 membranes annealed at 200ºC for various periods of time. It is shown that the water content value, which decreases with annealing time until it reaches a low plateau, mirrors the ΔH value of the same samples. This confirms the idea of crystalline domains in Nafion® act as barriers to solvent swelling and indicates that although the degree of crystallinity is small in these thermally annealed Nafion® membranes, it may have a significant effect on important properties of the membranes.

II. Future Work

A. Other Methods of Controlling the Degree of Crystallinity in Nafion®

Solution and melt-processing[5-8] can be used as a method of Controlling the Degree of Crystallinity in Nafion®. In solution processing, variables, such as solvent type, evaporation temperature, evaporation time, conterion type, can be controlled. Membranes processed under different conditions can be compared in order to find out optimal processing conditions. Melt-processing can be carried out using PFSIs containing various inorganic and organic counterions. Also, results from the crystallization kinetics study presented in this thesis may serve as guide for determining processing parameters like annealing time and temperature. Other methods, such as mechanical orientation[9], can also be considered.

B. Morphological Characterization of the Crystalline Component in Perfluorosulfonate Ionomers

Characterization methods other than DSC can be used to obtain more information regarding the extent and nature of the crystallinity in PFSI membranes. While the WAXD analysis results presented in this thesis fail to offer more insight into the isothermal crystallization process, perhaps due to the very small degrees of crystallinity in the samples, SAXS and SANS may be used to characterize the annealed membranes. SAXS and SANS might also offer information on the possible link between the crystallites and the organization of the ionic domains. ^{19}F and ^{13}C solid-state NMR (SSNMR) can be used to obtain information about the conformational order within the crystalline domains[10]. Samples with different degrees of crytallinity can be examined in the hope of assigning spectral features to crystallinity in the membrane and correlating these morphological features to site dynamics.

C. Investigation of the Morphology-Property Relationships in PFSI Membranes

Stress relaxation and creep experiments can be carried out in order to investigate mechanical properties of the membranes with different degrees of crystallinity. Dynamic mechanical analysis (DMA) will also be performed over a temperature range that covers the three mechanical relaxations, α, β and γ, with special attention to the α-relaxation, which is attributed to the onset of a dynamic electrostatic network[11]. Also, the in-plane proton conductivities of different membranes can be determined by impedance measurements using a four-point conductivity cell. The trend in proton conductivity with a change in the degree of crystallinity can then be evaluated. These results may be able to serve as guidance in the manipulation the morphology of PFSIs in order to yield desired membrane properties as well as improved PEMFC performance.

References

1. Park, J. K. Ph.D. Dissertation **2009**, Virginia Tech.
2. Alizadeh, A.; Richardson, L.; Xu, J. ; McCartney, S.; Marand, H.; Cheung, Y. W.; Chum, S. *Macromolecules* **1999**, *32*, 6221-6235.
3. Sohn, S.; Alizadeh, A.; Marand, H. *Polymer* **2000**, *41*, 8879-8886.
4. Huang, Z. Y.; Marand, H.; Cheung, W. Y.; Guest, M. *Macromolecules* **2004**, *37*, 9922-9932.
5. Yeo, S. C.; Eisenberg, A. *J. Appl. Polym. Sci.* **1977,** *21*, 875-898.
6. Moore, R. B.; Martin, C. R. *Anal. Chem.* **1986,** *58*, 2569-2570.
7. Moore, R. B.; Cable, K. M.; Croley, T. L. *J Membrane Sci* **1992,** *75*, 7-14.
8. Phillips, A. K.; Moore, R. B. *J. Polym. Sci. Pt. B-Polym. Phys.* **2006,** *44*, 2267-2277.

9. Page, K. A.; Landis, F. A.; Phillips, A. K.; Moore, R. B. *Macromolecules* **2006,** *39*, 3939-3946.

10. Chen, Q.; Schmidt-Rohr, K. *Macromolecules* **2004,** *37*, 5995-6003.

11. Page, K. A.; Cable, K. M.; Moore, R. B. *Macromolecules* **2005,** *38*, 6472-6484